Clim. Past Discuss., doi:10.5194/cp-2016-135, 2016
Manuscript under review for journal Clim. Past
Published: 21 December 2016

Hydroclimate of the Last Glacial Maximum and deglaciation in southern Australia's arid margin interpreted from speleothem records (23-15 ka)

Pauline C. Treble[1,2*], Andy Baker[2], Linda K. Ayliffe[3], Timothy J. Cohen[4], John C. Hellstrom[5], Michael K. Gagan[3], Silvia Frisia[6], Russell N. Drysdale[7], Alan D. Griffiths[1] and Andrea Borsato[6]

[1]Australian Nuclear Science and Technology Organisation, Lucas Heights 2234 NSW, Australia
[2]Connected Waters Initiative Research Centre, UNSW Australia, Kensington 2052 NSW, Australia
[3]Research School of Earth Sciences, Australian National University, Canberra ACT 0200, Australia
[4]School of Earth and Environmental Sciences, University of Wollongong, Wollongong NSW 2522, Australia
[5] School of Earth Sciences, University of Melbourne, Parkville VIC 3052, Australia
[6]School of Environmental and Life Science, University of Newcastle, Callaghan NSW 2308, Australia
[7]School of Geography, University of Melbourne, Parkville VIC 3052, Australia

*Corresponding author: pauline.treble@ansto.gov.au

Abstract

Terrestrial data spanning the Last Glacial Maximum (LGM) and deglaciation from the southern Australian region are sparse, and limited to discontinuous sedimentological and geomorphological records with relatively large chronological uncertainties. This dearth of records has prevented a critical assessment of the role of the Southern Hemisphere mid-latitude westerly winds on the region's climate during this time period. In this study, two precisely-dated speleothem records for Mairs Cave, Flinders Ranges, are presented, providing a detailed terrestrial hydroclimatic record for the southern Australian drylands during 23-15 ka for the first time. Enhanced recharge to Mairs Cave is interpreted from the speleothem record by the activation of growth, physical flood layering and $\delta^{18}O$ and $\delta^{13}C$ minima. Periods of lowered recharge are indicated by isotopic enrichment, primarily affecting $\delta^{18}O$, argued to be driven by evaporation of shallow soil/epikarst water in this water-limited environment. A hydrological driver is supported by calcite fabric changes.

The Mairs Cave record indicates that the Flinders Ranges were relatively wet during the LGM and early deglaciation, particularly over the interval 18.9-16 ka. This wetter phase ended abruptly with a shift to drier conditions at 15.8 ka. These findings are in agreement with the geomorphic archives for this region, as well as the timing of events in records from the broader Australasian region. The recharge phases identified in the Mairs Cave record are correlated with, but antiphase to, the position of the westerly winds interpreted from a marine core in the Great Australian Bight. The implication is that the mid-latitude westerlies are located further south during the period of enhanced recharge in the Mairs Cave record (18.9-16 ka), and conversely are located further north when greater aridity is interpreted in the speleothem record. A comparison with speleothem records from the northern Australasian region reveals that the availability of sub-tropical/tropical moisture is the most likely explanation driving enhanced recharge, with further amplification of recharge occurring during the early half of Heinrich Stadial 1, possibly influenced by a more southerly-displaced Intertropical Convergence Zone (ITCZ). A rapid transition to aridity at 15.8 ka is consistent with a retraction of this tropical moisture source.

Keywords: speleothem, Mairs Cave, Southern Australia, Heinrich Stadial 1, Last Glacial Maximum, westerly winds, recharge

Clim. Past Discuss., doi:10.5194/cp-2016-135, 2016
Manuscript under review for journal Clim. Past
Published: 21 December 2016

1. Introduction

The nature and timing of climatic episodes such as Heinrich Stadial 1 (HS1) in the Southern Hemisphere mid-latitudes during the last deglaciation is of high interest owing to the potential role of the westerly winds in driving CO_2 ventilation from the Southern Ocean and the impact of its release on global warming (Anderson et al., 2009; Cheng et al., 2010; Denton et al., 2010; Lamy et al., 2010; McGlone et al., 2010; Putnam et al., 2010; Lee et al., 2011; Broecker et al., 2012; Waugh et al., 2013). The latitudinal position of the westerly winds at the Last Glacial Maximum (LGM) is also an important research question which still remains debated despite long-running attention, both specifically in the southern Australian sector (Bowler 1978; Bowler and Wasson 1984; Wywroll et al. 2000; Shulmeister et al., 2004; Shulmeister et al., 2016; Williams et al., 2009; Hesse et al., 2004; Turney et al., 2006; Haberlah et al., 2010; Cohen et al., 2011; DeDeckker et al., 2012); and elsewhere in the Southern Hemisphere (Gasse et al., 2008; Sime et al., 2013).

Modelling and paleoclimate studies have proposed that the Southern Hemisphere westerly winds react to North Atlantic forcing, by contracting polewards during Heinrich Stadials, via feedback from a more southerly displaced Intertropical Convergence Zone (ITCZ) (Denton et al., 2010; Hodgson et al., 2010; Lee et al., 2011; Putnam et al., 2013). Critical assessment of this in the paleoclimate record is challenging, as reliable terrestrial paleoclimate records from the Southern Hemisphere mid-latitudes remain sparse (Broecker et al., 2012). More records, from key locations, are required to provide information regarding the exact timing and hydrological response of different regions, to contribute to the assessment of how the climate system reacts to solar insolation, sea level, CO_2 levels and feedbacks in the ocean/atmosphere system (Clark et al., 2012). Indeed, a compilation by Kohfeld et al. (2013) has shown that the global proxy data for the LGM suggests that an overall strengthening of the westerlies via an equatorward displacement is plausible, but that an alternative interpretation of no change in the westerlies at the LGM is also consistent with the proxy observations.

Currently, only a single proxy record exits for the position and strength of the westerly-winds from within the Australian sector (DeDeckker et al., 2012). Marine core MD03-2611 (33-10 ka) in the Great Australian Bight (GAB; Fig. 1a), is located at the present position of the Subtropical Front (STF). The paleo-position of the STF is interpreted from the micro-fossil (foraminifera), which in turn is used to infer the position and strength of the westerly-winds (DeDeckker et al., 2012). Several latitudinal excursions of the westerlies with winds extending further north than their Holocene position during the peak of the LGM, but further south during HS1, are interpreted from this record (DeDeckker et al., 2012). A key assumption of this study is that the position of the westerly winds coincides with the position of the oceanic STF, which may be a potential shortcoming (e.g. de Boer et al., 2013). A way of further assessing this interpretation is to examine the hydrological response to latitudinal shifts in the westerly winds in the terrestrial record of southern Australia.

Southern Australia is dominated by semi-arid drylands that skirt the southern margin of Australia's arid interior. The proximity to the arid interior means that it is hydrologically sensitive to episodes of climatic change (Fitzsimmons et al., 2013). Current terrestrial data that span the LGM and the subsequent deglaciation are particularly sparse in this region, and limited to discontinuous sedimentological and geomorphological archives (e.g. salt lakes, dune systems, ephemeral fluvial systems, etc.). Such records typically carry large chronological uncertainties due to preservation issues (e.g. lack of organic material, reworking of sediments, erosion) as well as the limitations of applicable age measurement techniques (Fitzsimmons et al., 2013). Additionally, the interpretation of geomorphic records may not be straightforward for other reasons. For example, dune activation may respond non-linearly to precipitation and be a function of sediment supply as well as aridity (Fitzsimmons et al., 2013); whilst the generally large catchments of Australia's arid interior contributes uncertainty over whether fluvial systems are recording local or distal conditions. For example, Lake Frome receives water from a catchment of nearly 63,000 km^2 with 44% of this contributing area drained by the adjacent Flinders Ranges and the rest from the adjacent dunefields (Cohen et al., 2012). Furthermore, connections with lakes Blanche and Callabonne mean that when Strzelecki Creek flows (via the tropically-sourced Cooper Creek) the contributing area of Lake Frome can actually be > 363,000 km^2.

Speleothems offer a number of advantages over the geomorphic archives described above, including i. having a relatively small catchment, hence are recorders of local recharge, ii. relatively good preservation of material in stable cave environments; iii. precise and accurate chronologies based on U-series age measurements by multi-collector inductively-coupled mass spectrometry (MC-ICPMS) typically resulting in age uncertainties of <1% (2σ; Hellstrom 2003); and iv. modern micro-milling and mass spectrometry techniques routinely produce sub-decadally resolved climatically-sensitive geochemical records spanning 10^3-10^4 year timescales (e.g. Wang et al., 2001; Griffiths et al., 2016). For example, over glacial-interglacial transitions in monsoonal climates, they have been particularly successful in showing the terminations (Cheng et al., 2010) and have placed speleothems at the forefront of chosen tools for paleoclimate reconstruction (Henderson et al., 2006; Fairchild and Baker, 2012).

Cave monitoring studies have shown dripwater $\delta^{18}O$ to be primarily a function of rainfall $\delta^{18}O$ in non-arid environments (e.g. Fuller et al., 2008; Moerman et al., 2013; Riechelmann et al., 2011; Treble et al. 2013; Duan et al., 2016) although the complexity of the climate-speleothem $\delta^{18}O$ signal is also recognised owing to karst hydrological pathways (Baker and Brunsdon, 2003; Treble et al., 2013), recharge thresholds (Pape et al., 2010; Markowska et al., 2015), and in-cave effects including disequilibrium during degassing, due to evaporation, and ventilation effects (e.g. Pape et al., 2010; Feng et al., 2012; Deininger et al., 2012; Cuthbert et al., 2014a,b; Riechelmann et al., 2013; Dreybrodt and Deininger, 2014; Rau et al., 2015).

Cave monitoring studies and speleothem records in general are primarily focused on temperate or tropical environments. Far less monitoring has been undertaken within semi-arid/arid climates (with the exception of Ayalon et al., 1998; Pape et al., 2010; Cuthbert et al., 2014a,b; Markowska et al., 2016). In these drier landscapes, where there is less frequent recharge, and temperatures conducive to evaporation occur, one would expect evaporative processes to increasingly affect dripwater $\delta^{18}O$, hence speleothem $\delta^{18}O$, with increasing aridity. Speleothem growth itself is typically episodic within semi-arid climates (Ayliffe et al., 1998; Wang et al. 2004; Vaks et al. 2006; Stoll et al., 2013). Recent studies from Wellington Caves in semi-arid central New South Wales, Australia, have contributed substantially to a process-based understanding of the climate-speleothem signal in water-limited environments. Cuthbert et al. (2014a,b) showed that dripwater $\delta^{18}O$ may be dominated by evaporation of water held in karst stores, occurring in between recharge events, and that significant recharge thresholds are needed to be overcome to replenish karst water stores (Markowska et al., 2016). These processes are likely to amplify the dripwater isotopic response to infiltration events, as well as introducing potential shifts in the frequency-magnitude relationships. On the whole, speleothem records from water-limited systems can be expected to have a considerable range in isotopic values, as well as a heightened non-linear relationship between climate and the speleothem isotopic record (Cuthbert et al. 2014a).

There has been relatively little use of speleothem records to reconstruct southern Australia's dryland history. To date, just three speleothem stable isotope records exist for this region (Desmarchelier et al., 2000; Bestland and Rennie, 2006; Quigley et al., 2010) from marine isotope stages 6 and 5d, and the Holocene; but all are of particularly low-resolution and contain lengthy millennial-duration hiatuses. Previous research has produced age measurements of speleothems from caves in this region, including Naracoorte, the Flinders Ranges and Kangaroo Island (Fig. 1a), resulting in age-frequency histograms (Ayliffe et al., 1998; St Pierre et al., 2012; Cohen et al., 2011; 2012). These studies highlight that speleothem growth in the southern margin of Australia's drylands is primarily a function of water balance, with enhanced speleothem growth coinciding with intervals of potentially greater moisture availability (Ayliffe et al., 1998; St Pierre

Clim. Past Discuss., doi:10.5194/cp-2016-135, 2016
Manuscript under review for journal Clim. Past
Published: 21 December 2016

et al., 2012; Cohen et al., 2011; Fitzsimmons et al., 2013). For example, the first such study by Ayliffe et al. demonstrated that speleothem growth at Naracoorte Caves is more frequent in the stadial periods of the last glacial cycle. This was attributed to higher recharge owing to reduced evapotranspiration.

A more recent study highlighted the climatic relationship between speleothem growth and pluvial intervals in this region via the overlap of two stalagmite records from Mairs Cave in the Flinders Ranges with lake-full conditions at Lake Frome, 200 km NE of the cave site, and fed by run-off from the eastern slopes of the Flinders Ranges (Cohen et al., 2011). This relationship between enhanced speleothem growth during periods of reduced evapotranspiration is also observed outside Australia (e.g. Wang et al. 2004; Vaks et al. 2006; Stoll et al., 2013) and highlights stalagmite growth as a useful on/off indicator of recharge in semi-arid to arid environments.

In this study, we present the geochemical records of these two stalagmites from Mairs Cave. As it was not practical to monitor Mairs Cave owing to its remote location, lack of active dripwater, and infrequent recharge, we compare our data with the modern analogue study at Wellington caves, in a temperate semi-arid environment 1000 km NE of Mairs Cave (Fig. 1). We also draw on a comparison of our data with independent evidence for the location of the westerly winds, inferred from the foraminifer-derived proxy record of the STF from marine core MD03-2611 in the GAB (DeDeckker et al., 2012), as well as other archives of climatic change relevant to the southern Australian region.

2. Regional setting

Today, the Flinders Ranges and surrounding region are classified as semi-arid to arid, and speleothem growth in the isolated pockets of Cambrian-age limestone karst is very sparse. The Flinders Ranges are a rugged 400 km long topographic divide intercepting the path of the westerly-winds from the Southern Ocean, providing orographically enhanced rainfall in a region otherwise characterised by flat, arid dunefields and large salt lakes (Figure 1a).

Rainfall at Mairs Cave is predominantly derived during winter months (Fig. 1c) but recharge in typical years is small to negligible, explaining the lack of modern speleothem growth. The region experiences limited connectivity with tropical moisture sources, owing to its position on the southern limb of the Hadley Cell, although the development of continental troughs during summer months can favour advection of moisture from the eastern Indian Ocean or Coral Sea (Figure 1a) and generate heavy summer rains (Schwerdtfeger and Curran, 1996; Pook et al., 2014). These extreme rainfall events often occur in negative Indian Ocean

Clim. Past Discuss., doi:10.5194/cp-2016-135, 2016
Manuscript under review for journal Clim. Past
Published: 21 December 2016

Dipole (IOD) events that coincide with La Niña years Negative IOD events occur when sea surface temperatures in the Eastern tropical Indian Ocean are warmer than average, feeding moisture into Australia's interior (Risbey et al., 2009). The interaction with frontal and low-pressure systems embedded in the westerly winds (e.g. complex-front type systems described by Pook et al., 2014) may result in significantly above average rainfall to southern and eastern Australia.

The 1974 filling of Lakes Frome and Callabonna is one of the most significant episodes in the historical record and happened in a year when a La Niña coincided with negative IOD. The lakes were fed both by direct runoff from the Flinders Ranges and from rain further north, via Strzelecki Creek (Cohen et al., 2011; 2012). During a single week-long event rainfall totals were broken across much of the arid interior. Persistent rainfall was generated by sustained moist tropical airflow. Moisture came from the eastern Indian Ocean for the first four days and then switched to the western Pacific Ocean, as shown by trajectory analysis (Figure 1d).

2.1 Mairs Cave

Mairs Cave (138º50'E, 32º10'S; Fig. 1b) is located in Buckalowie Gorge in the central Flinders Ranges. The cave is developed along three parallel bedding planes in the limestone (Kraehenbuehl, et al., 1997). Its overall length is 400 m although the main chamber is 120 m long by 10 m wide accessed via a 17 m vertical pitch at the cave entrance (Kraehenbuehl et al., 1997; Fig. 1c). Mairs Cave contains both coffee-coloured and clean white speleothem formation. Bands of coffee-coloured stalagmites lie underneath limestone joints, many overgrown with clean white formation.

3. Materials and methods

The two stalagmites used in this study were collected from Mairs Cave (Figure 1b) in 1998. MC-S1 was collected from the main chamber ~100 m into the cave and MC-S2 from a side chamber located ~20 m from the vertical shaft forming the cave entrance. There is evidence of flooding in the lower parts of Mairs Cave including calcite 'pool-formed decoration' as well as reports from cavers. for example, 3 m of water was reported in the entrance shaft in 1974 after the particularly heavy period of rain described in Section 2 (Kraehenbuehl, et al., 1997). There is no geomorphic evidence of streamflow inside the cave. The base of the entrance shaft is presently at a similar level to the creek but floodwaters are unlikely to be delivered to the cave via overbank flow from rising creek levels, as they would have to overtop >15 m which seems unlikely given the broad cross-section of the valley at this location. Alternatively, flooding may be caused by runoff from the steep terrain above the cave entrance.

Clim. Past Discuss., doi:10.5194/cp-2016-135, 2016
Manuscript under review for journal Clim. Past
Published: 21 December 2016

3.1 Description of stalagmites

The two stalagmites are considerably different in appearance (Figs. 2a,b). MC-S1 is darker 'coffee-coloured' (Fig. 2a) and contains well-defined parallel laminae appearing throughout the specimen (Fig. 2c), consisting of columnar and open-columnar fabric (Frisia et al., 2000). The growth surface of MC-S1 was wide and flat-topped, with gour features along the stalagmite flanks indicative of high dripwater Ca concentrations and high drip rate, of unknown duration and frequency. The coffee-colour is also indicative of organics, which would suggest more rapid connectivity to the soil than MC-S2. MC-S1 was sawn from a flowstone-covered boulder, approximately 10-15 mm of its base was not recoverable.

Stalagmite MC-S2 is pale, semi-translucent, and forms a narrow candle-stick stalagmite in its upper half. It contains thin lenses of calcite alternating with layers of calcified sediment in the lower half (Fig. 2b). This lower section captures the earliest growth phase of MC-S2, when calcite deposition competed with aggradation of sediment on the floor of the cave where MC-S2 grew (Fig. 2b). These sediment layers are more prominent and thicker in the lowest half of MC-S2, but are still visible on the stalagmite flanks between ~25-45 mm below the top. Sediment layers above this (upper 25 mm) appear to be absent, suggesting that either: i. sediment became more efficiently washed from the surface of MC-S2 as the morphology of its flanks became increasingly steeper; or ii. a cessation in sediment delivery to the floor where MC-S2 grew. The differences in the morphology of the two stalagmites indicates that this may be a function of drip rate: while both stalagmites are flat-topped with parallel bands, MC-S1 is twice as wide and has distinctive gour features on its sides, more commonly seen in flowstone, and indicative of higher drip rate (Baldini, 2001). The different morphologies indicate individual hydrological flow paths which can impact the geochemical record also (e.g. Bradley et al., 2010).

The sediment contained in these bands is assumed to be deposited by floodwaters, which is consistent with reports of water flooding the lower reaches of Mairs Cave. Judged from the cave maps (Hill, 1958), MC-S2 was located 30 m from and at a similar depth to the base of the entrance shaft. The shaft was reportedly flooded to a depth of 3 m in 1974 and MC-S2 was thus likely to have been inundated during this event. In contrast, MC-S1 grew ~4 m higher in elevation, 100 m from the entrance, and contains no sediment layers.

3.2 Methods

Two 5 mm slabs were sectioned longitudinally from each stalagmite. One slab was further sectioned along the longitudinal axis for stable isotopes and trace element analyses, while the ~8 mm wide portion from the central axis of the second slab was removed for age measurements. Calcite wafers, typically 1-2 mm thick, were further sub-sampled for age measurements. Adjacent surfaces were utilised to minimise potential offsets in the depths of measurement transects for stable isotope, trace element and age measurements.

Powders were obtained for stable isotope analysis via continuous micro-milling at 300 and 100 μm for MC-S1 and MC-S2 respectively, yielding sub-decadal resolution (approximately 5 years for the majority of each stalagmite; milling dimensions parallel to laminae were 2x2 mm for MC-S1 and 2x4 mm for MC-S2). The earliest visible lens of MC-S2 growth (Fig. 2c) was not included in the isotopic record owing to chronological uncertainty for this part of the record and detrital contamination (see Sect 4.1). Speleothem MC-S1 powders were analysed for $\delta^{18}O$ and $\delta^{13}C$ on a Finnegan MAT251 at the Research School of Earth Sciences (RSES), Australian National University, whilst MC-S2 powders were run on a GV2003 continuous-flow IRMS at the University of Newcastle. Data are normalised to the Vienna Peedee Belemnite (VPDB) scale using NBS-19 ($\delta^{18}O$=-2.20‰ and $\delta^{13}C$=+1.95‰) and NBS-18 ($\delta^{18}O$=-23.0‰ and $\delta^{13}C$=-5.0‰). The long-term measurement precision for NBS-19 at RSES is 0.07‰ (2σ) for $\delta^{18}O$ and 0.04‰ (2σ) for $\delta^{13}C$. Reproducibility between instruments was cross-checked by running aliquots of fifteen MC-S1 powders on each instrument resulting in <0.2‰ offset ($\delta^{18}O$ and $\delta^{13}C$). Initially every third sample was run and subsequent analyses were run to in-fill the time-series as necessary. Spectral analysis of $\delta^{18}O$ data was performed using the Lomb-Scargle method for unevenly sampled data (Press and Rybicki, 1989).

Trace elements were analysed by laser ablation inductively coupled plasma mass spectrometry (LA-ICPMS) at RSES, Australian National University, using a 193 nm excimer laser masked by slit that resulted in a rectangular area ablated from the sample surface that was 120 μm wide and 40 μm high aligned with the narrower dimension in the direction of speleothem growth. The sample was moved underneath the laser on a motorised stage at 2 mm/min while the laser is pulsed at 20 Hz such that the laser 'scanned' along the central growth axis of the speleothem. The ablated material was carried to an Agilent 7500s quadrupole ICPMS and the elements Ca, Mg, Sr, U, Al and Si analysed and standardised to using NIST 612 concentrations (Mg: 85.09, Sr: 78.4, Al: 10588, U: 37.88; Pearce et al., 1996). Full details of the LA-ICPMS procedure and data reduction are given in Treble et al. (2003). Construction of a proxy record of the sedimentary layers using Al and Si concentrations was attempted, but this was not successful due to the uneven distribution of sediment across the layers, and the tendency for sediments to be present on the stalagmite flanks rather than the axis. Instead the location of sediment bands was identified in thin section.

Clim. Past Discuss., doi:10.5194/cp-2016-135, 2016
Manuscript under review for journal Clim. Past
Published: 21 December 2016

The petrographic observations were carried out on uncoated, polished thin sections under plane (PPL) and cross-polarised light (XPL) using a Zeiss Axioskop optical microscope and a Leica MZ16A stereomicroscope at the University of Newcastle. Fabric coding and microstratigraphic logging follow a conceptual framework proposed in Frisia (2015), which is based on models of fabric development (Frisia et al., 2000). The microstratigraphic logs were tied to the stable isotope and age measurement slabs by using high-resolution scans of both thin sections and polished slabs.

The Al and U concentration data (not shown) were used as a broad guide to select calcite with low-detrital and highest U content for age measurements. Both stalagmites were examined in thin section and fabric and possible dislocations in growth were documented and also used to guide sub-sampling for age measurements. U-Th age measurements were conducted at the University of Melbourne following the methods of Hellstrom (2003; Table 1). Briefly, samples of 20-120 mg were dissolved in concentrated HNO_3 and equilibrated with a mixed ^{229}Th–^{233}U tracer. U and Th were extracted in a single solution using Eichrom TRU resin before introduction to a Nu Plasma multi-collector ICPMS where isotope ratios of both elements were measured simultaneously. Initial [$^{230}Th/^{232}Th$] was defined via modelling the age and depth data for MC-S2 and determined to be 0.58±0.29 and its uncertainty fully propagated for both stalagmite age models using Monte Carlo simulation of equation 1 of Hellstrom (2006). The method for the age-depth model is described in Hendy et al. (2012) and Scholz et al. (2012). The decay constants of Cheng et al. (2013) were used. Detrital content is low for MC-S1 resulting in negligible corrections of <0.4%. Corrections for MC-S2 were variable (0.1-5.4%) depending on proximity to sediment layers. Nine of the nineteen ages used to construct the Mairs Cave chronology appeared in Cohen et al. (2011) and are updated in Table 1 for completeness.

4. Results

4.1 Speleothem Chronology

The Mairs Cave speleothem record presented here is dated by a total of nineteen high-precision U-series disequilibrium age measurements (Table 1; Fig. 2a,b) and collectively spans 24 to 15 ka. A lens of calcite formed at the base of MC-S2 at 24.2 ka that was subsequently covered by sediment, before calcite recommenced growing at 23 ka. The exact growth interval of this lower lens could not be constrained with further age measurements owing to the amount of detrital material visible in this section. Age modelling shows that MC-S2 grew relatively slowly at 20 μm/a between 24.2 ka and 18.9 ka. Taking into account potential additional accretion by sediment layers suggests growth in this section (Fig. 2b)

Clim. Past Discuss., doi:10.5194/cp-2016-135, 2016
Manuscript under review for journal Clim. Past
Published: 21 December 2016

Climate of the Past
Discussions

may have been slower or possibly episodic, although age measurements made immediately either side of crystal growth dislocations identified in thin section, were found to be within error (Fig. 3a,c), suggesting that any suspension of growth was not for any significant duration. Thus the short-lived peaks in growth rate at 19 and 20.6 ka (Fig. 3b) are artifacts produced by the age-model on closely-spaced age measurements. MC-S2 growth slowed to 3 μm/a at 17.7 ka until growth terminated at 15.6+0.6/-1.6 ka, based on extrapolation of the 3rd and 97th percentile of the age-depth model to the top of the speleothem. This uncertainty largely reflects the slow growth rate through this section.

MC-S1 growth was initiated by 17.2 ka at a moderate growth rate (60-90 μm/a) until 15.8 ka, when growth decreased tenfold until it terminated at 14.9 ka (Fig. 3b). It should be noted that the beginning of this phase may have begun earlier (i.e. approximately 17.6 ka extrapolated from growth rate) as the very oldest portion of MC-S1 was not able to be sampled (Section 3.1). Overall, MC-S1 grew approximately 10 times faster than MC-S2.

4.2 Calcite fabric in thin sections

Both stalagmites are comprised predominately of columnar calcite. The compact columnar fabric of MC-S2 is, in its lower part (pre-20.6 ka) punctuated by several (>20) thin detrital layers, most evident on the flank of the stalagmite. Calcite re-nucleation and geometric selection occurs above the detritus rich layer. However, growth of the dominant forms mostly occurred in optical continuity with the substrate. In the upper 40 mm (post-20.6 ka) the sediment layers cease to drape over the growth axis although sediment lenses are still evident on the flank of the stalagmite up until ca. 18.9 ka. In this portion of the stalagmite, the fabric is compact columnar calcite and lamination is not visible or extremely faint.

By comparison, MC-S1 fabric is characterised by both compact, translucent and open, milky columnar subtypes with well-defined laminae (Fig. 2). The laminae are particularly well defined by the presence of brown organic-rich calcite from the base to 6 mm below the top (i.e. 17.2-15.6 ka; Fig. 3c). A further distinction of the fabrics has been applied on the basis of the shape of the crystal tips, which range from flat to rhombohedral. Such distinction allows an immediate recognition of the original thickness of the film of fluid bathing the stalagmite tip (Frisia, 2015) and has been, therefore, deemed an important characteristic of the stalagmite stratigraphy. Occurrence of rhombohedral tips, in fact, points to a thicker film of fluid, and thus higher recharge. Flat laminae suggest a thinner film thickness, thus reduced recharge with respect to the rhombohedral terminations. Typically, laminae group in bundles with flat or rhombohedral tips (Fig. 3). The thickness of the bundles ranges from approximately 400 to 1200 μm. Within these bundles, laminae are approximately 20-80 μm thick, suggesting that they may be sub-annual to annual features, judged against the mean growth rate of MC-S1 through this section, although their thickness is erratic with time.

4.3 Mairs Cave speleothem records

4.3.1 Speleothem $\delta^{18}O$

MC-S1 and MC-S2 $\delta^{18}O$ data spanning 23.2-14.9 ka are shown in Figure 3d. Considering the longer MC-S2 record, mean $\delta^{18}O$ is 0.3‰ lower than the long-term mean (-5.7‰) during 23.2-22.0 ka and close to the mean from 22-18.9 ka (Fig. 3d). In the interval of 23.2-18.9 ka, the $\delta^{18}O$ record contains multi-decadal to centennial variability of up to 2.5‰ that dominates over longer-term variability (Fig. 3d). This shorter-term variability is characterised by rapid transitions to isotopic minima that are relatively short-lived (typically 20-70 years), separated by longer intervals (50-200 years) of higher values, often displaying a rising trend, i.e. forming a saw-tooth type pattern. Post-18.9 ka, MC-S2 $\delta^{18}O$ is 0.2‰ lower than the mean until ~16.5 ka, during which the shorter-term variability is relatively dampened. This is not an artefact of sampling resolution as MC-S2 growth rate through this transition is constant (Fig. 3b). Afterwards, $\delta^{18}O$ rises above the mean by 0.2‰ overall, until MC-S2 growth ceases at 15.6 ka.

The shorter duration but faster growing MC-S1 record is approximately 0.5‰ lower compared with MC-S2 during the overlapping growth period (17.2 – 15.6 ka) during which MC-S1 is dominated by decadal isotopic variability of 1-1.5‰ (Fig. 3d). To compare the records more closely, a smoothing spline was applied to MC-S1 $\delta^{18}O$ data reducing its resolution over the common growth interval with MC-S2 by a factor of four. MC-S1 contains millennial-scale oscillations of approximately 1‰, defined by relatively short-lived minima. Several of these features align with similar features in the MC-S2 record but a close comparison is hampered by the relatively poorer precision of the MC-S2 chronology over this interval. At 15.8 ka, MC-S1 $\delta^{18}O$ rises 1‰ coinciding with the tenfold decrease in growth rate (Fig. 3b,d). Post-15.8 ka, MC-S1 $\delta^{18}O$ is 0.5‰ higher than the overall mean apart from a brief trough at 15.3 ka. MC-S1 terminates at 14.9 ka with a relatively high $\delta^{18}O$ value of -5.3‰.

4.3.2 Speleothem $\delta^{13}C$ and its relationship with $\delta^{18}O$

Mean MC-S2 $\delta^{13}C$ is particularly high (-0.9‰), being 7.1‰ more enriched than MC-S1 overall (Figure 3e). Prior to 18.9 ka, there are broad similarities with the $\delta^{18}O$ record, with MC-S2 $\delta^{13}C$ typically lower than the long-term mean until 22 ka and typically higher from 22 to 18.9 ka (Figure 3e). MC-S2 $\delta^{13}C$ is also characterised by multi-decadal to centennial variability that is equivalent or larger in magnitude (1-2‰) than millennial trends. In almost all cases, prominent $\delta^{18}O$ minima coincide with $\delta^{13}C$ minima but the relationship between the two isotopes appears to weaken between troughs. Maxima occasionally exceed 0‰ ($\delta^{13}C$) particularly between 20 and 18.9 ka (Figure 3e). Trends in MC-S2 $\delta^{13}C$ depart from $\delta^{18}O$ after 18.9 ka, with $\delta^{13}C$ declining approximately 2‰ until 17.7 ka, before rising again towards the termination of this record.

With respect to millennial trends, MC-S1 $\delta^{13}C$ rises from 17.2 to 16.8 ka, coinciding with rising values in MC-S2, but returns to lower values between 16.4 to 15.8 ka. MC-S1 $\delta^{13}C$ sharply rises by 2.5‰ at 15.8 ka, typically remaining high during this period of slow growth, apart from the reversal that also coincides with the $\delta^{18}O$ trough at 15.3 ka. Similar to the $\delta^{18}O$ record, MC-S1 $\delta^{13}C$ is characterised by multi-decadal isotopic variability of approximately 1‰ i.e. similar or lower in magnitude versus $\delta^{18}O$. As for the MC-S2 record, troughs in both isotopes coincide with regards to timing.

Scatter plots (Fig. 4a) show that MC-S2 $\delta^{18}O$ and $\delta^{13}C$ are moderately correlated during the earlier growth phase of 23.2-18.9 ka (r=0.7, slope 1.2), weaker during 18.9-17.6 ka (r=0.3, slope 0.5), and moderately correlated again during 17.6-15.5 ka (r=0.6, slope 1.2) (Fig. 4b,c). A correlation between $\delta^{18}O$ and $\delta^{13}C$ may indicate isotopic disequilibrium at the time of speleothem deposition (Hendy and Wilson, 1968). We note that MC-S2 shows no isotopic enrichment between axial and off-axis transects (13 mm apart; Figure S1), in either of the growth phases 23.2-18.9 or 17.6-15.5 ka, suggesting that calcite precipitation across the top of the stalagmite growth is occurring close to isotopic equilibrium. We note also that the high-frequency isotopic variability is often as large, or larger, in magnitude for $\delta^{18}O$ as for $\delta^{13}C$. Typically, kinetic effects result in C isotopic enrichment dominating O by about a factor of 2-4 (Fantidis and Ehhalt, 1970; Hendy, 1971; Mickler et al., 2006).

4.3.3 Spectral analysis of short-term $\delta^{18}O$ variability

A notable characteristic present in each of the speleothem isotopic records is the coincident troughs in both isotopes defining a saw-tooth pattern, particularly in regards to $\delta^{18}O$. The magnitude of these transitions can be up to several per mil with regards to $\delta^{18}O$ or $\delta^{13}C$ and is isotopically larger than millennial trends. Spectral analysis was conducted on MC-S1 (17.2-15.8 ka; post-15.8 ka was excluded due to low resolution of these data) and MC-S2 (23.0-16.0 ka) $\delta^{18}O$ records (Fig. 5a,b). The sole statistically-significant peak in MC-S1, at 187±15 years, is also present and significant in MC-S2 at 171±15 years. The uncertainty in the spectral peak locations was estimated by propagating the 2s error of age measurements at the ends of each record. MC-S2 exhibits a richer spectrum, with periods that are multiples of ~180, including one near 360 years which is perhaps the fundamental of the ~180 year peak, as well as an additional periodicity at ~133±15 a. The 180±15 a cycles persist through the 18.9 ka transition in the record, verified by repeating the spectral analysis on segments either side of 18.9 ka (not shown).

4.3.4 Mairs Cave speleothem Mg/Ca and Sr/Ca

Speleothem mean Mg/Ca and Sr/Ca ratios are higher in MC-S2 versus MC-S1 (Mg/Ca: 9.5 vs 2.7 mmol/mol; Sr/Ca: 0.29 vs 0.23 mmol/mol; Fig. 3f-g). There are similarities with the isotopic record, namely lower ratios prior to 22 ka, a decrease in ratios at 18.9 ka, and higher ratios towards the termination of the records from 16-15.8 ka onwards. The last observation is clearest in the case of Mg/Ca, where ratios become 50-200% higher. MC-S2 Mg/Ca contains a rising trend that coincides with rising $\delta^{13}C$ from 18 ka onwards.

MC-S2 Mg/Ca also contains decadal to centennial variability that is more prominent prior to 18.9 ka, but these features are less clear than the saw-tooth pattern observed in the isotopic record (Fig. 3d-e). These features are almost entirely absent in the MC-S1 Mg/Ca record (Fig. 3f), suggesting that the multi-decadal to centennial isotopic variability cannot fully be a product of post-infiltration karst processes.

With regards to Sr/Ca, there is better agreement between speleothem records in terms of mean Sr/Ca values (15% offset vs 72% offset for Mg/Ca) and possibly also centennial-millennial trends. There are higher Sr/Ca values in both speleothems 17-16.6 ka, coinciding with higher $\delta^{13}C$, and prominent shorter-lived maxima from 16 ka onwards appearing in both speleothems, but the chronological uncertainty in MC-S2 prevents direct correlation. Post-18.9 ka, Sr/Ca also declines to a minimum at 17.5-17.7 ka coinciding with a minimum in $\delta^{13}C$.

The relationship between speleothem Mg/Ca and Sr/Ca can be used to diagnose PCP. According to a theoretical derivation, the slope of ln(Mg/Ca) vs ln(Sr/Ca) should equal 0.88±0.13 if PCP is dominating (Sinclair et al., 2012). In these datasets, calculated slopes were close to zero, as there were no consistent relationships between these two variables in either speleothem (r = 0 to -0.1 over all key periods of interest; Supplementary Figure S2). This suggests that PCP is not dominating one or either of these elements. To investigate this further, we calculated the predicted variation in Mg/Ca, due to PCP, based on Sr/Ca variability. From Sinclair et al. (2012), if PCP is dominating both elements, then $\Delta\ln(Sr/Ca)/\Delta\ln(Mg/Ca) = 0.88$ (weight ratio). One s.d. of our ln(Sr/Ca) data is 0.16, thus the equivalent predicted variability in ln(Mg/Ca) would be just 0.18, which is approximately 13 times smaller (in mmol/mol units) compared with 1 s.d. of our measured ln(Mg/Ca) values (0.47). Similarly for MC-S1, the measured variability is 10 times greater than predicted by the PCP relationship. Hence, these calculations suggest that some other process is dominating any potential PCP signal in our data, and that this process has a greater impact on our Mg/Ca versus our Sr/Ca signal. This suggests that the Mg/Ca signal is complex at this site, consistent with the likelihood that Mg has multiple sources. This is consistent with other karst studies in Australia in water-limited regions where there are a greater number of identified sources and modifying processes for Mg (sea salt, dust, clay sorption, bedrock, biomass) compared to Sr, which has been found to be dominated by bedrock and dust alone (e.g. Goede et al., 1998; Rutlidge et al., 2014; Treble et al., 2016).

Further detailed comparison with the isotopic record was attempted, to tease out potential drivers such as soil processes, dilution, and autochthonous versus allochthonous sources. For example, lowered Mg/Ca coinciding with declining $\delta^{13}C$ and lower $\delta^{18}O$ from 19 to 18 ka could indicate a declining aeolian source during a period of soil stabilisation. The decline in aeolian contribution is also suggested by the progressive decrease of the detrital and re-nucleation layers from 23.0 ka to 20.6 ka and their disappearance after 18.9 ka, i.e. a reduction in supply. Further detailed analyses, probably requiring a larger suite of trace elements, may be carried out in a future study to fully investigate this. In this present study, we simply draw from the broad similarities between Mg/Ca, Sr/Ca and the isotopic record for i. the multi-decadal to centennial-scale variability prior to 18.9 ka; ii. the transition at 18.9 ka; and iii. the rise in these signals after 15.8 ka, to argue that these features are broadly hydrologically-driven.

5. Discussion

5. 1. Mairs Cave stalagmites as a record of groundwater recharge

<u>5.1.1. Isotopic disequilibrium as an indicator of recharge during 23-18.9 ka</u>

There are several characteristics that suggest that isotopic disequilibrium is impacting the Mairs Cave speleothem record and that this impact varies through time and spatially between stalagmites: i. MC-S2 is isotopically enriched compared with MC-S1; ii. relatively slow growing MC-S2 has particularly high mean $\delta^{13}C$ overall (-0.9‰); and iii. $\delta^{18}O$ and $\delta^{13}C$ are moderately correlated during the earlier growth phase 23-18.9 ka (r=0.7).

Typically, isotopic disequilibrium is considered to be caused by either i. fractionation during the degassing process enhanced by high dripwater supersaturation and slow drip rates (Fantidis and Ehhalt, 1970; Day and

Henderson, 2011); or ii. fractionation driven by within-cave evaporation, from either low relative humidity and or high ventilation (Deininger et al., 2012). We can expect several of these to be more common in semi-arid karst settings (e.g. low drip rates, low cave air relative humidity, Cuthbert et al., 2014a). However, it appears that the calcite has precipitated closer to isotopic equilibrium across the top of stalagmite MC-S2 (Sect. 4.3.2). This suggests isotopic disequilibrium could be occurring in the parent dripwaters; for example, by incomplete equilibration or evaporation in the soil/epikarst karst stores (Bar-Matthews et al. 1996; Cuthbert et al., 2014a). The fact that variability in $\delta^{18}O$ is as large or larger than for $\delta^{13}C$ (Sect. 4.3.2), strongly supports that significant evaporation of the soil/epikarst waters occurred.

We argue that the impact of recharge is also evident in the multi-decadal to centennial variability, which appear as saw-tooth type features displaying rapid 1-2.5‰ decreases in $\delta^{18}O$, separated by longer periods of ^{18}O-enrichment, often reaching a maxima immediately before an abrupt transition into a trough. The $\delta^{18}O$ minima typically coincide with $\delta^{13}C$ troughs, and occur throughout a period of relatively elevated mean $\delta^{13}C$ (Fig. 3d,e). This is consistent with a model of infiltration-driven disequilibrium effects in a semi-arid karst environment, with: i. $\delta^{18}O$ minima representing times of recharge when dripwater is least fractionated by evaporation in the soil/vadose zone and/or in the cave (as recharge stimulates faster dripping), and ii. $\delta^{13}C$ minima are related to increased soil CO_2 bioproductivity and/or less fractionation. The $\delta^{18}O$ variation is consistent with isotopic modification of dripwaters of up to 2‰ observed during monitoring of a modern semi-arid environment at Wellington Caves (Cuthbert et al., 2014a).

The persistence of sediment bands representing cave floor flooding, and the occasional dissolution feature identified via thin section in the 18.9-23 ka interval of MC-S2, further support a hydrological driver, i.e. that the cave is affected by intermittent recharge. The dissolution features implicate undersaturated dripwaters, possibly via rapid infiltration of high intensity events resulting in soil zone bypass or inundation by floodwaters.

5.1.2 Recharge during the LGM

The abrupt shift in the isotopic records at 18.9 ka, coinciding with the peak of the LGM, is characterised by: i. a 2‰ abrupt decrease in both $\delta^{18}O$ and $\delta^{13}C$; ii. reduced isotopic amplitude, and iii. weak co-variation between $\delta^{18}O$ and $\delta^{13}C$; that persists for at least several millennia (Fig. 3d,e). Based on the above proposed infiltration/disequilibrium model, the isotopic data suggest a shift in hydrological regime to more effective recharge and/or reduced evapotranspiration from 18.9 ka until 15.8 ka. The dampening of the $\delta^{18}O$ signal suggests enhanced storage of dripwater aided by relatively greater recharge. Enhanced recharge is also supported by the coincident reduction in Mg/Ca ratios (Fairchild and Treble, 2009; Tremaine and Froelich, 2013; Belli et al., in press).

The absence of sediment bands in MC-S2 after 18.9 ka could also suggest a hydrological change, although we cannot exclude that this is simply a function of the stalagmite growth outpacing streamwater levels or a reduction in sediment supply. MC-S1 began growing by 17.2 ka during this proposed period of enhanced recharge. Initiation of a new stalagmite suggests activation of a new flow path, further supporting more effective recharge. The occurrence of bundles of laminae showing parallel versus rhombohedral-tipped layers suggests that the increase in effective recharge varied, periodically, from 17.2 to 16.2 ka (Fig. 3c), with episodes of dissolution (highest recharge of understaturated waters) between 16.7 and 16.2 ka. The presence of laminae indicates input of colloidal particles during infiltration when water was at its lowest supersaturation state (Frisia et al., 2003). The occurrence itself of the visible organic colloids, would suggest that maximum infiltration occurred in a cooler context (Frisia et al., 2003), which prevented efficient organic matter degradation. From 15.7 ka (Fig. 3b) the columnar calcite is fully closed (1 on fabric log) and laminae are either absent or faint. This suggests that there was less input of colloidal natural organic matter from the soil zone.

Our spectral analysis demonstrates that multi-decadal to centennial variability in speleothem $\delta^{18}O$ persists through the LGM and early deglaciation. Speleothem $\delta^{18}O$ can be related to rainfall characteristics such as rainfall amount, moisture source and/or trajectory effects, and this has been examined in the modern record for southwest Australia, located at similar latitudes to Mairs Cave (Treble et al., 2005; Fischer and Treble, 2008). It may be tempting to interpret this multi-decadal variability in the Mairs Cave $\delta^{18}O$ record as being directly related to rainfall isotopic variability e.g. such as our 1974 modern analogue (Sect. 2) during which particularly low rainfall isotopic values were recorded in Adelaide (-10‰ compared with precipitation-weighted annual mean of -4.5‰; IAEA/WMO, 2006) owing to the 'continental effect' (Welker, 2000). However, we consider that in a semi-arid environment, moisture source variation cannot be reliably fingerprinted owing to the additional isotopic impact of evapotranspiration and non-linear karst hydrological effects. Thus, while the precise cause of the isotopic variability in this dataset is unknown, it has to be related to recharge and water balance.

A final point to raise when considering mean speleothem $\delta^{18}O$ during the LGM, is that cave temperature and ice-volume would also have had an impact on these values. We modelled this following Griffiths et al., 2009 (Fig. S3). This suggested speleothem $\delta^{18}O$ was a further ~2‰ lower at 18.9 ka compared with 16 ka. However, such a figure is probably a maximum and cannot realistically be constrained, as other factors impact precipitation $\delta^{18}O$. For example, a cooler LGM atmosphere would counteract isotopic depletion, as well as the isotopic impact of evapotranspiration and atmospheric source/trajectory effects. We note the fact that millennial variation is isotopically smaller than the decadal-centennial variation suggests that in any case, it does not exceed the hydrological uncertainty in the Mairs Cave speleothem isotopic record.

5.1.3. Shift to aridity at 15.8 ka

15.8 ka marks a transition in the Mairs Cave record evidenced by an abrupt +1‰ step-shift in MC-S1 $\delta^{18}O$ and +2.5‰ in $\delta^{13}C$ (Figure 3d,e). This is accompanied by higher Mg/Ca values, an almost 10-fold reduction in growth rate, and the shift towards closed columnar fabric without lamination (Fig. 3b-c,f). Furthermore, this also occurs approximately at the time of overall isotopic enrichment and higher Mg/Ca in the MC-S2 record, followed by termination of MC-S2 growth (given the chronological uncertainty; Fig. 3a,d-f). The response of these variables is consistent with a drying signal. A similar response was observed during a multi-decadal drought period recorded in a modern speleothem in the southern Australian region (Treble et al., 2005a) and elsewhere (Asrat et al., 2007). The shift to aridity at 15.8 ka in the Mairs Cave record is a particularly robust signal given the multiple lines of evidence i.e. termination of MC-S2 and the abrupt shift in hydrologically-sensitive proxies in MC-S1. Termination of MC-S1 at (~14.9 ka) is consistent with the impact of persistent drying, possibly resulting from depletion or loss of connectivity with the shallow vadose water store feeding MC-S1.

5.2 Comparison of Mairs Cave record with other archives

5.2.1 Regional geomorphology records

The Mairs Cave record overlaps chronologically with a nearby hydrologically-sensitive archive, the 'Flinders silts' record from the western side of the central Flinders Ranges (Callen 1983; Haberlah et al., 2010) approximately 100 km from Mairs Cave. The Flinders silts date from ~24 to ~16 ka and consist of thick sequences (up to 18 m) of slackwater laminae forming upstream of narrow gorges. These fine-grained silts, originally blown from a deflated Lake Torrens to the west, were fluvially re-worked and deposited by back-flooding of narrow gorges beginning 47 ka until 16 ka (Haberlah et al., 2010). Laminae are interpreted to represent rapid deposition from floods with approximately centennial frequency during 24-19 ka, with storms interpreted to have reduced in frequency and/or magnitude after 19 ka, and termination of flood laminae at 16 ka.

The Mairs Cave and Flinders silts records correlate remarkably well in terms of their timing of hydrological change with a "switching on" of recharge at 24 ka and "switching off" at 16 ka and a significant change in the hydrological characteristics at 19 ka. However, they differ somewhat in the interpretation of the hydrological change at 19 ka, i.e. reduced storm frequency/intensity in the silt record versus more effective recharge in the stalagmite record. Although speculative, combining this evidence may indicate something of the nature of this change in terms of the frequency/magnitude characteristics of the rainfall i.e. a shift to more frequent, lower magnitude events leading to more continuous recharge, or the speleothem isotopic record may just reflect reduced evapotranspiration over this interval. The records do agree in the 23-19 ka interval in terms of significant hydrological events of approximate centennial frequency, i.e. high-magnitude floods in the silts record are consistent with significant recharge occurring approximately every 130-180 years in the Mairs Cave record.

We note here, also, that it was previously unresolved whether the termination of Flinders silts at 16 ka was due to a lack of floods or the exhaustion of silt supply (Haberlah et al., 2010). However, the match with the abrupt transition to aridity in our data supports a climatic driver for the termination of the floodwater lamina.

Increased hydrologically effective precipitation in the 19-16 ka period is also supported by OSL-ages from beachridges at Lake Frome (Fig. 1a) indicating that it was 15-20 times the modern volume between 18-16 ka (Cohen et al., 2011; 2012) coincident with relatively high levels of charcoal and woodland taxa pollen present in the sediments of the lake floor (Singh and Luly, 1991; Luly, 2001). The shift to aridity at 15.8 ka in Mairs Cave is supported by significant reductions in *Callitris* sp pollen and charcoal (Singh and Luly, 1991). Fluvial records for the Goulburn, Lachlan and Gwydir catchments also indicate a wetter LGM interval (although the timing is either variable between catchments or lacks precision (Bowler, 1978; Kemp and Rhodes, 2010; Peitsch et al., 2013). The Strzelecki dune fields to the north and east of the Flinders Ranges (Fig. 1a) record an interval of pedogenesis (indicating relative stability) from ~19 ka, followed by a major phase of dune reactivation ~15-14 ka (Fitzsimmons et al., 2009). Evidence for a high lake phase at Lake Mungo (Willandra Lakes system) was also recently reported but dated to 24 ka (Fitzsimmons et al., 2015).

5.2.2 Comparing Mairs Cave with the Great Australian Bight marine record

Comparing the Mairs Cave record with the GAB marine record (DeDeckker et al., 2012) reveals that the transitions identified in the STF record also coincide

Clim. Past Discuss., doi:10.5194/cp-2016-135, 2016
Manuscript under review for journal Clim. Past
Published: 21 December 2016

remarkably with those at Mairs Cave in terms of timing i.e. 19 and 16 ka (Fig. 6b). However, we highlight the following inconsistency. The GAB STF record is interpreted as a proxy of westerly winds, with the westerlies interpreted to have shifted *further* from Australia between 19-16 ka. This implies a *reduction* in moisture from the westerlies during the same interval during which, we interpret an *increase* in recharge to the Flinders Ranges. Further to this, at 16 ka, the marine record indicates that the westerlies have shifted closer to Australia and even further *north* of their Holocene location, implying restored westerly airflow over southern Australia, at the same time that we observe a shift to aridity. The GAB quartz record, interpreted as an indicator of aeolian activity over southern Australia, implies a reduction in aridity after 18 ka. This is somewhat consistent with the Mairs Cave record, although nearly 1000 years later in terms of timing.

These observations raise an interesting problem: that the Mairs Cave record, which is sensitive to recharge, appears to be hydrologically out of tune with the evidence in the marine record. We explore three possibilities for the disagreement in the marine and terrestrial records:

I. SSTs in the Southern Ocean were more important for moisture delivery rather than mean latitudinal position of the westerlies;
II. the water balance was sensitive to temperature (i.e. evaporation) rather than simply rainfall (5.2.3); or
III. rainfall to Mairs Cave was dependent on another moisture source other than the westerlies (5.2.4).

Addressing the first point, we note that the ~4°C rise in GAB SST from 18 to 16 ka (Fig. 6c) would boost the moisture originating from the Southern Ocean, possibly providing a relative increase in rainfall even if the GAB record implies that air masses from the Southern Ocean crossed the Flinders Ranges less frequently. However, the SST rise doesn't commence until 18 ka, ~1000 years later than the shift to increased recharge in the Flinders Ranges commencing at 18.9 ka. Additionally, SSTs stay high for the remainder of the record, whereas the Mairs Cave stalagmites provide strong support for a shift to aridity at 15.8 ka. These two observations argue against Southern Ocean SSTs being a primary driver.

5.2.3 Increased recharge due to reduced evapotranspiration

Addressing the second point, it was shown previously (Williams et al., 2006) that recharge to the Flinders Ranges at the LGM could be enhanced simply because evaporation would be reduced in a cooler environment (Williams et al., 2006). We demonstrate this also, by using the Thornthwaite method to estimate evaporation (Thornthwaite, 1948). Figure 1c shows calculations of monthly hydrologically effective precipitation (HEP) for: i. present day monthly rainfall and temperature in the Flinders Ranges; and ii. LGM temperatures, whereby monthly temperature was offset by -6°C and -10°C consistent with a range of estimates given for LGM temperature lowering in southern Australia (Galloway, 1965; Miller et al., 1997). Although simplistic, this calculation demonstrates the potential for a significant increase in recharge when potential evaporation is lowered (between four and six-fold) with potential recharge occurring at 25-50% of today's monthly rainfall. This further suggests that there is opportunity for recharge to be generated by lower magnitude events. That is, given that monthly recharge typically occurs via infrequent events, it suggests recharge could be generated at the LGM by events that are approximately half the magnitude required for recharge today, which would also occur more frequently. However, terrestrial temperatures were likely cooler through the whole of the LGM period. This explanation could be responsible for the presence of speleothem growth throughout the 23-16 ka period, but does not appear consistent with the relatively abrupt shift to enhanced recharge at 18.9 ka which requires an additional mechanism.

5.2.4 Comparing Mairs Cave with monsoon speleothem records

Thirdly, we consider whether effective precipitation may be higher if the region is being watered from systems other than the westerlies. There is evidence that northern Australia and southern Indonesia may have been wetter during parts of the Last Termination and this has been linked to changes in the Indo-Australian Summer Monsoon (IASM) activity/Western Pacific Warm Pool (WPWP) dynamics and/or a southward shift in the ITCZ (e.g. Nott and Price, 1994; English et al., 2001; Turney et al., 2004; Denniston et al., 2013a; Ayliffe et al. 2013). Figure 6f shows the speleothem records from Ball Gown Cave in NW Western Australia (Fig. 1a; Denniston et al., 2013a) and the Liang Luar records (Fig. 6e) from Flores, Indonesia (Fig. 1a; Ayliffe et al., 2013). A more southward displaced ITCZ could increase the availability of tropical moisture to the higher latitudes; although according to these studies, the timing of the ITCZ displacement coincides with the onset of HS1 which is at least 1000 years later than the onset of the relatively wetter interval at Mairs Cave (18.9 ka) although consistent with the highest interval of recharge in the MC-S1 record (<17.2-15.8 ka) (Fig. 6a). See Section 5.3.5 for further discussion.

The record from C126 Cave in Cape Range, Western Australia, is also shown (Fig 6g; Denniston et al., 2013b). According to the speleothem records, both the Flinders Ranges and Cape Range are experiencing increased recharge during 19-16 ka. This could support that both sites were affected by a common driver. At Cape Range, the driver of $\delta^{18}O$ variability was unconstrained as this location is currently watered by moisture both from subtropical/tropical systems and mid-latitude westerlies, and these end members could not be separated isotopically

Clim. Past Discuss., doi:10.5194/cp-2016-135, 2016
Manuscript under review for journal Clim. Past
Published: 21 December 2016

(Denniston et al., 2013b). But given that both sites are receiving more recharge, and if the westerlies are further south during this interval as interpreted in the GAB record (Fig. 6b), it could be argued that a subtropical/tropical moisture source is the most plausible explanation.

In the modern record, the delivery of moisture from the warm seas surrounding northern Australia to its interior is strongly governed by tropical ocean patterns associated with the El Niño-Southern Oscillation (ENSO) and the Indian Ocean Dipole (IOD) (Ummenhofer et al., 2009). Variability in tropical Pacific and Indian Ocean SSTs, in particular, strongly influences southern Australian rainfall (Ummenhofer et al., 2009; Pook et al., 2014) and has been shown to display decadal variability (Ummenhofer et al., 2011). Reconstruction of coral-based archives further suggest that IOD and ENSO-like patterns also operate on decadal through to millennial timescales during the Holocene (e.g. Gagan et al., 2004; Abram et al., 2009; Moy et al., 2002) as well as other archives (e.g. Stott et al., 2002; Sarnthein et al. 2011). A more La Nina-like or negative IOD-like state in the glacial period has been previously invoked (e.g. Sarnthein et al., 2011; Muller et al., 2008). Further to this, GCM studies suggest that the Hadley Cell was reduced in strength in the subsidence regions during both the LGM (Sime et al., 2013) and HS1 (Lee et al., 2011), suggesting that a weakening of the sub-tropical ridge across Australia would permit deeper penetration of troughs into interior Australia.

5.2.5 HS1 in the Mairs Cave records

As noted above, there are some similarities with changes in the Mairs Cave record and speleothem records from the northern Australasian region (Ball Gown Cave and Liang Luar records; Fig. 6a, e-g). Both the Ball Gown Cave and the Liang Luar records are considered to be influenced by the intensity/location of the IASM with a more southerly-displaced IASM inferred during HS1 (Denniston et al., 2013; Ayliffe et al., 2013). While it's difficult to judge against the Ball Gown Cave record, given that the uncertainty in its chronology is approximately ±1 kyr at this point, $\delta^{18}O$ decreases at the onset of HS1 and rises again after 15 ka (Fig. 6f), which is approximately similar in timing to the period of highest recharge in the Mairs Cave record: 17.2±0.08 (or possibly ~0.4 kyr earlier, given MC-S1's earliest growth was not retrieved) to 15.8±0.07 ka. This interval also compares well with low $\delta^{18}O$ from 17.6±0.1 to 14.6±0.1 ka in the comparatively well-dated Flores record. It also agrees well, in terms of timing, with events recorded in other precisely dated archives outside of the Australasian region, interpreted as a response to HS1 e.g. Wang et al., 2001; Partin et al., 2007; Cheng et al., 2010 and others summarised in Naafs et al., (2013). There is thus good evidence that the enhanced recharge recorded during the same period at Mairs Cave is owing to further moisture availability from a southerly-displaced IASM during HS1.

As noted by Zhang et al. (2016), both the Flores and Ball Gown Cave records have low $\delta^{18}O$ troughs at 16 ka, implying wet conditions, but the trend in both records quickly reverses suggesting a weakening of the IASM followed from 16 to approximately 14.7 ka (Fig. 6f-g). The GAB marine record also suggests a northward displacement in the mid-latitude westerlies from 16 ka, implying a return of westerly airflow to the Flinders Ranges at the same time that Mairs Cave records an abrupt shift from wetter to drier conditions (Section 5.1.3). This combined evidence reinforces a tropical driver for enhanced recharge to the Flinders Ranges followed by an abrupt shift to aridity via the retraction of subtropical/tropical moisture and restored westerly airflow. This is feature in the Mairs Cave record is thus further evidence for the northward shift in the ITCZ interpreted in the monsoon speleothem records at the onset of the Bølling-Allerød (Ayliffe et al., 2013; Denniston et al., 2013a)

6. Conclusions

We consider the Mairs Cave stalagmites as a record of groundwater recharge to the Flinders Ranges over the LGM/early deglacial. Relative recharge is primarily indicated by the on/off activation of speleothem growth and degree of isotopic disequilibrium, supported by Mg/Ca values and calcite fabric changes. It appears that this interval, overall, was relatively wetter than previous or subsequent times, with the wettest phase between 19-16 ka, ending abruptly with a shift to drier conditions at 15.8 ka. Specifically, we have identified three phases within the 23-15 ka interval summarised as:

I. 23-18.9 ka: MC-S2 activates but shows isotopic disequilibrium driven by evaporation in the soil/epikarst water stores, punctuated with multi-decadal periods of higher effective recharge and cave flooding.

II. 19-15.8 ka: MC-S2 has reduced isotopic disequilibrium indicating increased infiltration and/or reduced evapotranspiration and MC-S1 activates due to relatively more recharge. Speleothem $\delta^{13}C$ is also relatively lower in each record, supporting enhanced soil bioproductivity in wetter/warmer soils above Mairs Cave.

III. 15.8 ka: MC-S1 records a shift to aridity, coinciding with the termination of MC-S2 and, eventually, MC-S1 growth indicating the end of effective recharge.

These findings agree well with other regional geomorphic evidence for high-magnitude floods of approximately centennial frequency in the Flinders silts (coinciding with phase I), lake highstands (coinciding with phase II) and re-activation of dunefields (overlapping phase III) in the southern Australian drylands. In comparison, the Mairs Cave record is the most precisely-dated and highest-resolution record of these archives to date, and the first able to confirm

Clim. Past Discuss., doi:10.5194/cp-2016-135, 2016
Manuscript under review for journal Clim. Past
Published: 21 December 2016

that recharge to this region is responding to key global events during the last Termination (LGM and HS1).

The source of moisture responsible for enhanced recharge could not be reliably isotopically fingerprinted for the Mairs Cave record, as it is within the hydrological uncertainty of the speleothem $\delta^{18}O$ data. However, comparing the Mairs Cave record with other records from further afield, notably the GAB marine record (westerly winds) and northwest Australian and Indonesian speleothem records (tropical systems), raises an intriguing possibility that wetter intervals in the southern Australian drylands appear to be more sensitive to the availability of subtropical/tropical moisture rather than the position of the westerly winds. Thus it appears that westerly rainfall may have been relatively ineffectual at driving recharge to southern Australia during the LGM. The latter challenges simple assumptions made previously in the geomorphology and Quaternary literature that wetter intervals in the interior of southern Australian paleo record during the last glacial imply westerly airflow as a driver e.g. Cohen, Haberlah et al., 2010, Fitzsimmons et al., 2013; and others.

The dependence of significant rainfall to the Australian interior on the availability of subtropical/tropical moisture associated with La Nina and/or negative IOD phases, is well established in modern climatology (e.g. Ummenhofer et al., 2009; 2011; Pook et al., 2014). Our interpretation of the recharge characteristics from the Mairs Cave isotopic record suggests that these important patterns influencing southern Australian rainfall, may have operated during the LGM and deglacial period. The ~180 a cycles persisted through the whole 23-16 ka interval, suggesting that the mechanism for multi-decadal variability in recharge (e.g. 1974 type events) was always available. Further to this, given that these cycles persist right through the 23-16 ka interval, other mechanisms may be amplifying recharge from 18.9 ka, particularly during HS1 e.g. Southern Ocean SST's, reduced evapotranspiration, a further increase in availability of tropical moisture from a more southerly displaced ITCZ during HS1, or some combination of these.

Data availability: Data from Figure 3 will be uploaded onto the NOAA Paleoclimatology database.

Competing interests: The authors declare that they have no conflict of interest.

Author contribution: PCT performed the stable isotope analyses for MC-S1 and the trace element analyses for both stalagmites as well as the majority of the data interpretation and manuscript drafting; JCH performed the U/Th dating; SF and A. Borsato performed the fabric log and thin section analysis; LA collected the speleothems; AG drafted Fig. 1d and 5; A. Baker, TJC, MKG and RND contributed to the interpretation and manuscript writing.

Acknowledgements

We would like to thank Rod Wells for the use of stalagmite MC-S2 and discussions about Mairs Cave; James Shulmeister, Pandora Hope, John Chappell, Ed Rhodes, Martin Williams, Ian Houshold and David Haberlah for discussions on the region's climate (both today and in the past) and geomorphology; as well as Monika Markowska for discussions on semi-arid speleothem records. We thank also Janece McDonald, Islay Laird, Krista Simon and Joan Cowley for assistance with milling and isotope analysis; Stuart Hankin for drafting Fig 1a,b; Patrick DeDeckker, Matthias Moros and Rhawn Denniston for supplying published data; and Dan Sinclair for discussions on quantifying PCP. The stable isotope measurements on MC-S1 and MC-S2 were supported by Australian Research Council LIEF grants LE0989624 and LE0668400, and U-Th age measurements by Australian Research Council LIEF grant LE0989067. The majority of the data were collected whilst PCT was a Research Fellow at the Australian National University.

Clim. Past Discuss., doi:10.5194/cp-2016-135, 2016
Manuscript under review for journal Clim. Past
Published: 21 December 2016

References

Abram, N. J., McGregor, H. V., Gagan, M. K., Hantoro, W. S., and Suwargadi, B. W.: Oscillations in the southern extent of the Indo-Pacific Warm Pool during the mid-Holocene, Quaternary Science Reviews, 28, 2794-2803, 2009.

Anderson, R.F., Ali, S., Bradtmiller, L.I., Nielson, S.H.H., Fleisher, M.Q., Anderson, B.E., Burckle, L.H.,: Wind-driven upwelling in the Southern Ocean and the deglacial rise in atmospheric CO2. Science 323, 1443-1448, 2009.

Asrat, A., Baker, A., Mohammed, M.U., Leng, M.J., Van Calsteren, P., Smith, C.,: A high-resolution multi-proxy stalagmite record from Mechara, Southeastern Ethiopia: palaeohydrological implications for speleothem palaeoclimate reconstruction. Journal Of Quaternary Science 22, 53-63, 2007.

Ayalon, A., Bar-Mathews, M., and Sass, E.: Rainfall-recharge relationships within a karstic terrain within the Eastern Mediterranean semi-arid region, Israel: d18O and dD charateristics, Journal of Hydrology, 207, 18-30, 1998.

Ayliffe, L.K., Marianelli, P.C., McCulloch, M.T., Mortimeter, G.E., Hellstrom, J.C., Moriarty, K.C., Wells, R.T.,: 500 ka precipitation record from southeastern Australia: Evidence for interglacial relative activity. Geology 26, 147-150, 1998.

Ayliffe, L.K., Gagan, M.K., Zhao, J.-x., Drysdale, R.N., Hellstrom, J.C., Hantoro, W.S., Griffiths, M.L., Scott-Gagan, H., St Pierre, E., Cowley, J.A. & Suwargadi, B.W.,: Rapid interhemispheric climate links via the Australasian monsoon during the last deglaciation. *Nature Communications* 4:2908 doi:10.1038/ncomms3908, 2013.

Baker, A. and Brunsdon, C.: Non-linearities in drip water hydrology: an example from Stump Cross Caverns, Yorkshire, Journal of Hydrology, 277, 151-163, 2003.

Baker, A. and Bradley, C.: Modern stalagmite $\delta^{18}O$; instrumental calibration and forward modelling, Global and Planetary Change, 71, 201-206, 2011.

Bar-Matthews, M, Ayalon, A., Matthews, A., Sass, E. and Halicz, L.,: Carbon and oxygen isotope study of the active water-carbonate system in a karstic Mediterranean cave: Implications for paleoclimate research in semiarid regions. Geochim. Cosmochim. Acta 60, 337-347, 1996.

Belli, R., Borsato, A., Frisia, S., Drysdale, R.N., Maas, R., & Greig, A. Investigating Mg and Sr hydrological significance through Sr isotopes and particulate elements analyses in stalagmites across the Lateglacial to Holocene transition. Geochim. Cosmochim. Acta, in press. DOI: 10.1016/j.gca.2016.10.024

Bestland, E. A. and Rennie, J.: Stable isotope record ($\delta^{18}O$ and $\delta^{13}C$) of a Naracoorte Caves speleothem (Australia) from before and after the Last Interglacial. , Alcheringa, Special Issue 1, 19-29, 2006.

Bowler, J. M. (Ed.): Quaternary climate and tectonics in the evolution of the Riverine Plain, southeastern Australia, ANU Press, Canberra, Australia, 1978.

Bowler, J. M. and Wasson, R. J.: Glacial age environments of inland Australia. In: Late Cainozoic palaeoclimates of the Southern Hemisphere, Vogel, J. C. (Ed.), Balkema, Rotterdam, 1984.

Bradley, C., Baker, A., Jex, C.N., Leng, M.J.,: Hydrological uncertainties in the modelling of cave drip-water d18O and the implications for stalagmite palaeoclimate recontructions. Quaternary Science Reviews 29, 2201-2214, 2010.

Broecker, W., Putnam, A.E.,: How did the hydrologic cycle respond to the two-phase mystery interval? Quaternary Science Reviews 57, 17-25, 2012.

Callen, R. A.: Quaternary climatic cycles, Lake Millyera region, southern Strzelecki Desert, Transactions of the Royal Society of South Australia, 108, 163-173, 1984.

Cuthbert, M. O., Baker, Andy, Jex, Catherine N., Graham, Peter W., Treble, Pauline C., Andersen, Martin S., Acworth, R. Ian: Drip water isotopes in semi-arid karst: implications for speleothem paleoclimatology, Earth and Planetary Science Letters, 395, 194-204, 2014a.

Cuthbert, M. O., Rau, G. C., Andersen, M. S., Roshan, H., Rutlidge, H., Marjo, C. E., Markowska, M., Jex, C. N., Graham, P. W., Mariethoz, G., Acworth, R. I., and Baker, A.: Evaporative cooling of speleothem drip water, Sci Rep-Uk, 4, 2014b.

Cheng, H., Edwards, R.L., Broecker, W.S., Denton, G.H., Kong, X., Wang, Y., Zhang, R., Wang, X., 2010. Ice age terminations. Science 326, 248-252.

Cheng, H., Edwards, R. L., Shen, C. C., Polyak, V. J., Asmerom, Y., Woodhead, J., Hellstrom, J., Wang, Y. J., Kong, X. G., Spotl, C., Wang, X. F., and Alexander, E. C.: Improvements in Th-230 dating, Th-230 and U-234 half-life values, and U-Th isotopic measurements by multi-collector inductively coupled plasma mass spectrometry, Earth and Planetary Science Letters, 371, 82-91, 2013.

Clark, P. U., Shakun, J. D., Baker, P. A., Bartlein, P. J., Brewer, S., Brook, E., Carlson, A. E., Cheng, H., Kaufman, D. S., Liu, Z. Y., Marchitto, T. M., Mix, A. C., Morrill, C., Otto-Bliesner, B. L., Pahnke, K., Russell, J. M., Whitlock, C., Adkins, J. F., Blois, J. L., Clark, J., Colman, S. M., Curry, W. B., Flower, B. P., He, F., Johnson, T. C., Lynch-Stieglitz, J., Markgraf, V., McManus, J., Mitrovica, J. X., Moreno, P. I., and Williams, J. W.: Global climate evolution during the last deglaciation, P Natl Acad Sci USA, 109, E1134-E1142, 2012.

Cohen, T. J., Nanson, G. C., Jansen, J. D., Jones, B. G., Jacobs, Z., Larsen, J. R., May, J. H., Treble, P., Price, D. M., and Smith, A. M.: Late Quaternary mega-lakes fed by the northern and southern river systems of central Australia: varying moisture sources and increased continental aridity, Palaeogeography, Palaeoclimatology and Palaeoecology, 356-357, 89-108, 2012.

Cohen, T.J., Nanson, G.C., Jansen, J.D., Jones, B.G., Jacobs, Z., Treble, P., Price, D.M., May, J.H., Smith, A.M., Ayliffe, L.K., C, H.J.,: Continenal aridification and the vanishing of Australia's megalakes. Geology 39, 167-170, 2011.

De Boer, A. M., Graham, R. M., Thomas, M. D., Kohfeld, K. E.,: The control of the Southern Hemisphere Westerlies on the position of the Subtropical Front, J. Geophys. Res. Oceans, 118, 5669–5675, doi:10.1002/jgrc.20407, 2013.

De Deckker, P., Moros, M., Perner, K., Jansen, E.,: Influence of the tropics and southern westerlies on glacial interhemispheric asymmetry. Nature Geoscience 5, 266-269, 2012.

Deininger, M., Fohlmeister, J., Scholz, D., and Mangini, A.: Isotope disequilibrium effects: The influence of evaporation and ventilation effects on the carbon and oxygen isotope composition of speleothems - A model approach, Geochimica et Cosmochimica Acta, 96, 57-79, 2012.

Denniston, R. F., Wyrwoll, K. H., Asmerom, Y., Polyak, V. J., Humphreys, W. F., Cugley, J., Woods, D., LaPointe, Z., Peota, J., and Greaves, E.: North Atlantic forcing of millennial-scale Indo-Australian monsoon dynamics during the Last Glacial period, Quaternary Science Reviews, 72, 159-168, 2013a.

Denniston, R. F., Asmerom, Y., Lachniet, M., Polyak, V. J., Hope, P., An, N., Rodzinyak, K., and Humphreys, W. F.: A Last Glacial Maximum through middle Holocene stalagmite record of coastal Western Australia climate, Quaternary Science Reviews, 77, 101-112, 2013b.

Denton, G. H., Anderson, R. F., Toggweiler, J. R., Edwards, R. L., Schaefer, J. M., and Putnam, A. E.: The Last Glacial Termination, Science, 328, 1652-1656, 2010.

Desmarchelier, J. M., Goede, A., Ayliffe, L. K., McCulloch, M. T., and Moriarty, K.: Stable isotope record and its palaeoenvironmental interpretation for a late Middle Pleistocene speleothem from Victoria Fossil Cave, Naracoote, South Australia, Quaternary Science Reviews, 19, 763-774, 2000.

Dreybrodt, W. and Deininger, M.: The impact of evaporation to the isotope composition of DIC in calcite precipitating water films in equilibrium and kinetic fractionation models, Geochim Cosmochim Ac, 125, 433-439, 2014.

Duan, W. H., Ruan, J. Y., Luo, W. J., Li, T. Y., Tian, L. J., Zeng, G. N., Zhang, D. Z., Bai, Y. J., Li, J. L., Tao, T., Zhang, P. Z., Baker, A., and Tan, M.: The transfer of seasonal isotopic variability between precipitation and drip water at eight caves in the monsoon regions of China, Geochim Cosmochim Ac, 183, 250-266, 2016.

English, P., Spooner, N. A., Chappell, J., Questiaux, D. G., and Hill, N. G.: Lake Lewis basin, central Australia: environmental evolution and OSL chronology, Quatern Int, 83-5, 81-101, 2001.

Fairchild, I. J. and Baker, A.: Speleothem Science: From process to past environments, Wiley-Blackwell, Oxford, 2012.

Clim. Past Discuss., doi:10.5194/cp-2016-135, 2016
Manuscript under review for journal Clim. Past
Published: 21 December 2016

Climate of the Past
Discussions
Open Access

Fairchild, I. J. and Treble, P. C.: Trace elements in speleothems as recorders of environmental change, Quaternary Science Reviews, 28, 449-468, 2009.

Fantidis, J. and Ehhalt, D.: Variations of the carbon and oxygen isotopic composition in stalagmites and stalactites: Evidence of non-equilibrium isotopic fractionation, Earth and Planetary Science Letters, 10, 136-144, 1970.

Feng, W. M., Banner, J. L., Guilfoyle, A. L., Musgrove, M., and James, E. W.: Oxygen isotopic fractionation between drip water and speleothem calcite: A 10-year monitoring study, central Texas, USA, Chemical Geology, 304, 53-67, 2012.

Fischer, M.J., Treble, P.C.,: Calibrating climate-delta O-18 regression models for the interpretation of high-resolution speleothem delta O-18 time series. Journal Of Geophysical Research-Atmospheres 113, D17103, 2008.

Fitzsimmons, K. E., Magee, J. W., and Amos, K. J.: Characterisation of aeolian sediments from the Strzelecki and Tirari Deserts, Australia: Implications for reconstructing palaeoenvironmental conditions, Sediment Geol, 218, 61-73, 2009.

Fitzsimmons, K. E., Cohen, T. J., Hesse, P. P., Jansen, J., Nanson, G. C., May, J. H., Barrows, T. T., Haberlah, D., Hilgers, A., Kelly, T., Larsen, J., Lomax, J., and Treble, P.: Late Quaternary palaeoenvironmental change in the Australian drylands, Quaternary Science Reviews, 74, 78-96, 2013.

Fitzsimmons, K. E., Stern, N., Murray-Wallace, C. V., Truscott, W., and Pop, C.: The Mungo Mega-Lake Event, Semi-Arid Australia: Non-Linear Descent into the Last Ice Age, Implications for Human Behaviour, Plos One, 10, 2015.

Frisia, S.: Microstratigraphic logging of calcite fabrics in speleothems as tool for palaeoclimate studies. Int. J. Speleol. 44, 1–16, 2015.

Frisia, S., Borsato, A., Fairchild, I. J., and McDermott, F.: Calcite fabrics, growth mechanisms and environments of formation in speleothems (Italian Alps and SW Ireland), Journal of Sedimentary Research, 70, 1183-1196, 2000.

Frisia, S., Fairchild, I.J., Fohlmeister, J., Miorandi, R., Spötl, C., & Borsato, A.: Carbon dioxide and carbon isotopes mass balance modelling in dynamic cave systems and implications for stalagmite capture of seasonal climate proxies. Geochimica et Cosmochimica Acta 75: 380–400, 2011.

Fuller, L., Baker, A., Fairchild, I. J., Spötl, C., Marca-Bell A., Rowe, P., and Dennis, P. F.: Isotope hydrology of dripwaters in a Scottish cave and implications for stalagmite palaeoclimate research, Hydrol. Earth Syst. Sci., 12, 1065-1074, 2008.

Gagan, M. K., Hendy, E. J., Haberle, S. G., and Hantoro, W. S.: Post-glacial evolution of the Indo-Pacific Warm Pool and El Nino-Southern Oscillation, Quatern Int, 118, 127-143, 2004.

Galloway, R. W.: Late Quaternary climates in Australia, The Journal of Geology, 73, 603-618, 1965.

Clim. Past Discuss., doi:10.5194/cp-2016-135, 2016
Manuscript under review for journal Clim. Past
Published: 21 December 2016

Climate of the Past
Discussions
Open Access

Gasse, F., Chalie, F., Vincens, A., Williams, M. A. J., and Williamson, D.: Climatic patterns in equatorial and southern Africa from 30,000 to 10,000 years ago reconstructed from terrestrial and near-shore proxy data, Quaternary Science Reviews, 27, 2316-2340, 2008.

Goede, A., McCulloch, M., McDermott, F., and Hawkesworth, C.: Aeolian contribution to strontium and strontium isotope variations in a Tasmanian speleothem, Chemical Geology, 149, 37-50, 1998.

Griffiths, M.L., Drysdale, R.N., Gagan, M.K., Frisia, S., Zhao, J., Ayliffe, L.K., Hantoro, W.S., Hellstrom, J.C., Fischer, M.J., Feng, Y., Suwargadi, B.W.,: Evidence for Holocene changes in Australian-Indonesian monsoon rainfall from stalagmite trace element and stable isotope ratios. Earth and Planetary Science Letters 292, 27-38, 2009.

Griffiths, M. L., Kimbrough, A. K., Gagan, M. K., Drysdale, R. N., Cole, J. E., Johnson, K. R., Zhao, J. X., Cook, B. I., Hellstrom, J. C., and Hantoro, W. S.: Western Pacific hydroclimate linked to global climate variability over the past two millennia, Nat Commun, 7, 2016.

Haberlah, D., Williams, M. A. J., Halverson, G., McTainsh, G. H., Hill, S. M., Hrstka, T., Jaime, P., Butcher, A. R., and Glasby, P.: Loess and floods: High-resolution multi-proxy data of Last Glacial Maximum (LGM) slackwater deposition in the Flinders Ranges, semi-arid South Australia, Quaternary Science Reviews, 29, 2673-2693, 2010.

Hellstrom, J.: U-Th dating of speleotherns with high initial Th-230 using stratigraphical constraint, Quaternary Geochronology, 1, 289-295, 2006.

Hellstrom, J.: Rapid and accurate U/Th dating using parallel ion-counting multi-collector ICP-MS, Journal of Analytical Atomic Spectrometry, 18, 1346-1351, 2003.

Henderson, G. M.: Caving in to new chronologies, Science, 313, 620-622, 2006.

Hendy, C.,: The isotope geochemistry of speleothems-I. The calculation of the effects of different modes of formation on the isotopic composition of speleothems and their applicability as palaeoclimatic indicators. Geochimica et Cosmochimica Acta 35, 802-824, 1971.

Hendy, C., Wilson, A.,: Palaeoclimatic data from speleothems. Nature 219, 48-51, 1968.

Hendy, E. J., Tomiak, P. J., Collins, M. J., Hellstrom, J., Tudhope, A. W., Lough, J. M., and Penkman, K. E. H.: Assessing amino acid racemization variability in coral intra-crystalline protein for geochronological applications, Geochim Cosmochim Ac, 86, 338-353, 2012.

Hesse, P. P., Magee, J. W., and van der Kaars, S.: Late Quaternary climates of the Australian arid zone: a review, Quatern Int, 118, 87-102, 2004.

Hill, A. L.,: Mairs Cave Buckalowie Creek, Australian Speleological Federation map no. 5F3-CEG1009, 1958.

Hodgson, D. A. and Sime, L. C.: Palaeoclimate Southern Westerlies and CO2, Nature Geoscience, 3, 666-667, 2010.

IAEA/WMO,: Global Network of Isotopes in Precipitation. The GNIP Database. Accessible at: http://www.iaea.org/water, 2006.

Kalnay, E., Kanamitsu, M., Kistler, R., Collins, W., Deaven, D., Gandin, L., Iredell, M., Saha, S., White, G., Woollen, J., Zhu, Y., Leetmaa, A., Reynolds, R., Chelliah, M., Ebisuzaki, W., Higgins, W., Janowiak, J., Mo, K. C., Ropelewski, C., Wang, J., Jenne, R., and Joseph, D.: The NCEP/NCAR 40-Year Reanalysis Project, Bulletin of the American Meteorological Society, 77, 437-471, 1996.

Kemp, J. and Rhodes, E. J.: Episodic fluvial activity of inland rivers in southeastern Australia: Palaeochannel systems and terraces of the Lachlan River, Quaternary Science Reviews, 29, 732-752, 2010.

Kohfeld, K. E., Graham, R. M., de Boer, A. M., Sime, L. C., Wolff, E. W., Le Quere, C., and Bopp, L.: Southern Hemisphere westerly wind changes during the Last Glacial Maximum: paleo-data synthesis, Quaternary Science Reviews, 68, 76-95, 2013.

Kraehenbuehl, P. et al.,: Caves of the Flinders Ranges. South Australian Speleological Council, Adelaide, 1997.

Lamy, F., Kilian, R., Arz, H. W., Francois, J. P., Kaiser, J., Prange, M., and Steinke, T.: Holocene changes in the position and intensity of the southern westerly wind belt, Nature Geoscience, 3, 695-699, 2010.

Luly, J. G.: On the equivocal fate of Late Pleistocene Callitris Vent. (Cupressaceae) woodlands in arid South Australia, Quatern Int, 83-5, 155-168, 2001.

Lee, S. Y., Chiang, J. C. H., Matsumoto, K., and Tokos, K. S.: Southern Ocean wind response to North Atlantic cooling and the rise in atmospheric CO2: Modeling perspective and paleoceanographic implications, Paleoceanography, 26, 2011.

Markowska, M., Baker, A., Treble, P. C., Andersen, M. S., Hankin, S., Jex, C. N., Tadros, C. V., and Roach, R.: Unsaturated zone hydrology and cave drip discharge water response: Implications for speleothem paleoclimate record variability, Journal of Hydrology, doi: http://dx.doi.org/10.1016/j.jhydrol.2014.12.044, 2015. 2015.

Markowska, M., Baker, A., Andersen, M. S., Jex, C. N., Cuthbert, M. O., Rau, G. C., Graham, P. W., Rutlidge, H., Mariethoz, G., Marjo, C. E., Treble, P. C., and Edwards, N.: Semi-arid zone caves: Evaporation and hydrological controls on delta O-18 drip water composition and implications for speleothem paleoclimate reconstructions, Quaternary Science Reviews, 131, 285-301, 2016.

McGlone, M. S., Turney, C. S. M., Wilmshurst, J. M., Renwick, J., and Pahnke, K.:

Clim. Past Discuss., doi:10.5194/cp-2016-135, 2016
Manuscript under review for journal Clim. Past
Published: 21 December 2016

Divergent trends in land and ocean temperature in the Southern Ocean over the past 18,000 years, Nature Geoscience, 3, 622-626, 2010.

Mickler, P. J., Stern, L. A., and Banner, J. L.: Large kinetic isotope effects in modern speleothems, Geological Society Of America Bulletin, 118, 65-81, 2006.

Miller, G., Magee, J., and Jull, A.: Low-latitude glacial cooling in the Southern Hemisphere from amino-acid racemization in emu eggshells, Nature, 385, 241-244, 1997.

Moerman, J. W., Cobb, K. M., Adkins, J. F., Sodemann, H., Clark, B., and Tuen, A. A.: Diurnal to interannual rainfall delta O-18 variations in northern Borneo driven by regional hydrology, Earth and Planetary Science Letters, 369, 108-119, 2013.

Moy, C. M., Seltzer, G. O., Rodbell, D. T., and Anderson, D. M.: Variability of El Nino/Southern Oscillation activity at millennial timescales during the Holocene epoch, Nature, 420, 162-165, 2002.

Muller, J., Kylander, M., Wust, R. A. J., Weiss, D., Martinez-Cortizas, A., LeGrande, A. N., Jennerjahn, T., Behling, H., Anderson, W. T., and Jacobson, G.: Possible evidence for wet Heinrich phases in tropical NE Australia: the Lynch's Crater deposit, Quaternary Science Reviews, 27, 468-475, 2008.

Naafs, B., Hefter, J., and Stein, R.: Millennial-scale ice rafting events and Hudson Strait Heinrich (-like) Events during the late Pliocene and Pleistocene: a review, Quaternary Science Reviews, 80, 1-28, 2013.

Nott, J. and Price, D.: Plunge Pools and Paleoprecipitation, Geology, 22, 1047-1050, 1994.

Orland, I. J., Burstyn, Y., Bar-Matthews, M., Kozdon, R., Ayalon, A., Matthews, A., and Valley, J. W.: Seasonal climate signals (1990-2008) in a modern Soreq Cave stalagmite as revealed by high-resolution geochemical analysis, Chem Geol, 363, 322-333, 2014.

Pape, J. R., Banner, J. L., Mack, L. E., Musgrove, M., and Guilfoyle, A.: Controls on oxygen isotope variability in precipitation and cave drip waters, central Texas, USA, Journal of Hydrology, 385, 203-215, 2010.

Pietsch, T. J., Nanson, G. C., and Olley, J. M.: Late Quaternary changes in flow-regime on the Gwydir distributive fluvial system, southeastern Australia, Quaternary Science Reviews, 69, 168-180, 2013.

Pearce, N. J. G., Perkins, W. T., Westgate, J. A., Gorton, M. P., Jackson, S. E., Neal, C. R., and Chenery, S. P.: A compilation of new and published major and trace element data for NIST SRM 610 and NIST SRM 612 glass reference materials, Geostandards Newsletter, 21, 115-144, 1996.

Pook, M. J., Risbey, J. S., Ummenhofer, C. C., Briggs, P. R., and Cohen, T. J.: A synoptic climatology of heavy rain events in the Lake Eyre and Lake Frome catchments, Frontiers in Environmental Science, 2, 1-8, 2014.

Press, W.H., Rybicki, G.B.,: Fast algorithm for spectral analysis of unevenly sampled data. The Astrophysical Journal 338, 277-280, 1989.

Putnam, A. E., Denton, G. H., Schaefer, J. M., Barrell, D. J. A., Andersen, B. G., Finkel, R. C., Schwartz, R., Doughty, A. M., Kaplan, M. R., and Schluchter, C.: Glacier advance in southern middle-latitudes during the Antarctic Cold Reversal, Nature Geoscience, 3, 700-704, 2010.

Putnam, A. E., Schaefer, J. M., Denton, G. H., Barrell, D. J. A., Andersen, B. G., Koffman, T. N. B., Rowan, A. V., Finkel, R. C., Rood, D. H., Schwartz, R., Vandergoes, M. J., Plummer, M. A., Brocklehurst, S. H., Kelley, S. E., and Ladig, K. L.: Warming and glacier recession in the Rakaia valley, Southern Alps of New Zealand, during Heinrich Stadial 1, Earth Planet Sc Lett, 382, 98-110, 2013.

Quigley, M. C., Horton, T., Hellstrom, J. C., Cupper, M. L., and Sandiford, M.: Holocene climate change in arid Australia from speleothem and alluvial records, Holocene, 20, 1093-1104, 2010.

Rau, G. C., Cuthbert, M. O., Andersen, M. S., Baker, A., Rutlidge, H., Markowska, M., Roshan, H., Marjo, C. E., Graham, P. W., and Acworth, R. I.: Controls on cave drip water temperature and implications for speleothem-based paleoclimate reconstructions, Quaternary Sci Rev, 127, 19-36, 2015.

Riechelmann, D. F. C., Schroder-Ritzrau, A., Scholz, D., Fohlmeister, J., Spotl, C., Richter, D. K., and Mangini, A.: Monitoring Bunker Cave (NW Germany): A prerequisite to interpret geochemical proxy data of speleothems from this site, Journal of Hydrology, 409, 682-695, 2011.

Riechelmann, D. F. C., Deininger, M., Scholz, D., Riechelmann, S., Schroder-Ritzrau, A., Spotl, C., Richter, D. K., Mangini, A., and Immenhauser, A.: Disequilibrium carbon and oxygen isotope fractionation in recent cave calcite: Comparison of cave precipitates and model data, Geochimica et Cosmochimica Acta, 103, 232-244, 2013.

Risbey, J. S., Pook, M. J., McIntosh, P. C., Ummenhofer, C. C., and Meyers, G.: Characteristics and variability of synoptic features associated with cool season rainfall in southeastern Australia, Int. J. Climatol., 29, 1595-1613, 2009.

Rutlidge, H., Baker, A., Marjo, C. E., Andersen, M. S., Graham, P. W., Cuthbert, M. O., Rau, G. C., Roshan, H., Markowska, M., Mariethoz, G., and Jex, C. N.: Dripwater organic matter and trace element geochemistry in a semi-arid karst environment: Implications for speleothem paleoclimatology, Geochim Cosmochim Ac, 135, 217-230, 2014.

Scholz, D., Hoffmann, D. L., Hellstrom, J., and Ramsey, C. B.: A comparison of different methods for speleothem age modelling, Quat Geochronol, 14, 94-104, 2012.

Schwerdtfeger, P. and Curran, E. (Eds.): Climate of the Flinders Ranges, Royal Society of South Australia, Adelaide, 1996.

Shulmeister, J., Goodwin, I., Renwick, J., Harle, K., Armand, L., McGlone, M. S., Cook, E., Dodson, J., Hesse, P. P., Mayewski, P., and Curran, M.: The Southern Hemisphere westerlies in the Australasian sector over the last glacial cycle: a synthesis, Quatern Int, 118, 23-53, 2004.

Shulmeister, J., Kemp, J., Fitzsimmons, K. E., and Gontz, A.: Constant wind regimes during the Last Glacial Maximum and early Holocene: evidence from Little Llangothlin Lagoon, New England Tablelands, eastern Australia, Climate of the Past, 12, 1435-1444, 2016.

Sime, L. C., Kohfeld, K. E., Le Quere, C., Wolff, E. W., de Boer, A. M., Graham, R. M., and Bopp, L.: Southern Hemisphere westerly wind changes during the Last Glacial Maximum: model-data comparison, Quaternary Science Reviews, 64, 104-120, 2013.

Sinclair, D. J., Banner, J. L., Taylor, F. W., Partin, J., Jenson, J., Mylroie, J., Goddard, E., Quinn, T., Jocson, J., and Miklavic, B.: Magnesium and strontium systematics in tropical speleothems from the Western Pacific, Chemical Geology, 294, 1-17, 2012.

Singh, G. and Luly, J.: Changes in Vegetation and Seasonal Climate since the Last Full Glacial at Lake Frome, South-Australia, Palaeogeogr Palaeocl, 84, 75-&, 1991.

St Pierre, E., Zhao, J. X., Feng, Y. X., and Reed, E.: U-series dating of soda straw stalactites from excavated deposits: method development and application to Blanche Cave, Naracoorte, South Australia, J Archaeol Sci, 39, 922-930, 2012.

Stoll, H. M., Moreno, A., Mendez-Vicente, A., Gonzalez-Lemos, S., Jimenez-Sanchez, M., Dominguez-Cuesta, M. J., Edwards, R. L., Cheng, H., and Wang, X. F.: Paleoclimate and growth rates of speleothems in the northwestern Iberian Peninsula over the last two glacial cycles, Quaternary Research, 80, 284-290, 2013.

Stott, L.: Super ENSO and global climate oscillations at millennial time scales (vol 297, pg 222, 2002), Science, 298, 751-751, 2002.

Sarnthein, M., Grootes, P. M., Holbourn, A., Kuhnt, W., and Kuhn, H.: Tropical warming in the Timor Sea led deglacial Antarctic warming and atmospheric CO2 rise by more than 500 yr, Earth Planet Sc Lett, 302, 337-348, 2011.

Thornthwaite, C. W.: An approach toward a rational classification of climate, Geographical Review, 38, 55-94, 1948.

Treble, P., Shelley, J.M.G., Chappell, J.,: Comparison of high resolution sub-annual records of trace elements in a modern (1911-1992) speleothem with instrumental climate data from southwest Australia. Earth And Planetary Science Letters 216, 141-153, 2003.

Clim. Past Discuss., doi:10.5194/cp-2016-135, 2016
Manuscript under review for journal Clim. Past
Published: 21 December 2016

Treble, P.C., Chappell, J., Gagan, M.K., McKeegan, K.D., Harrison, T.M.,: In situ measurement of seasonal delta O-18 variations and analysis of isotopic trends in a modem speleothem from southwest Australia. Earth And Planetary Science Letters 233, 17-32, 2005.

Treble, P.C., Bradley, C., Wood, A., Baker, A., Jex, C.N., Fairchild, I.J., Gagan, M.K., J, C., C, A.,: An isotopic and modelling study of flow paths and storage in Quaternary aeolinite, SW Australia: implications for speleothem paleoclimate records. Quatarnary Science Reviews 64, 90-103, 2013.

Treble, P. C., Fairchild, I. J., Griffiths, A., Baker, A., Meredith, K. T., Wood, A., and McGuire, E.: Impacts of cave air ventilation and in-cave prior calcite precipitation on Golgotha Cave dripwater chemistry, southwest Australia, Quaternary Sci Rev, 127, 61-72, 2015.

Treble, P. C., Fairchild, I. J., Baker, A., Meredith, K. T., Andersen, M. S., Salmon, S. U., Bradley, C., Wynn, P. M., Hankin, S., Wood, A., and McGuire, E.: Roles of forest bioproductivity, transpiration and fire in a nine-year record of cave dripwater chemistry from southwest Australia, Geochim Cosmochim Ac, 184, 132-150, 2016.

Tremaine, D. M. and Froelich, P. N.: Speleothem trace element signatures: A hydrologic geochemical study of modern cave dripwaters and farmed calcite, Geochimica et Cosmochimica Acta, 121, 522-545, 2013.

Turney, C. S. M., Kershaw, A. P., Clemens, S. C., Branch, N., Moss, P. T., and Fifield, L. K.: Millennial and orbital variations of El Nino/Southern Oscillation and high-latitude climate in the last glacial period, Nature, 428, 306-310, 2004.

Turney, C. S. M., Kershaw, A. P., Lowe, J. J., van der Kaars, S., Johnston, R., Rule, S., Moss, P., Radke, L., Tibby, J., McGlone, M. S., Wilmshurst, J. M., Vandergoes, M. J., Fitzsimons, S. J., Bryant, C., James, S., Branch, N. P., Cowley, J., Kalin, R. M., Ogle, N., Jacobsen, G., and Fifield, L. K.: Climatic variability in the southwest Pacific during the Last Termination (20-10 kyr BP), Quaternary Science Reviews, 25, 886-903, 2006.

Ummenhofer, C. C., England, M. H., McIntosh, P. C., Meyers, G. A., Pook, M. J., Risbey, J. S., Gupta, A. S., and Taschetto, A. S.: What causes southeast Australia's worst droughts?, Geophys Res Lett, 36, 2009.

Ummenhofer, C. C., Sen Gupta, A., Li, Y., Taschetto, A. S., and England, M. H.: Multi-decadal modulation of the El Nino-Indian monsoon relationship by Indian Ocean variability, Environ Res Lett, 6, 2011.

Vaks, A., Bar-Matthews, M., Ayalon, A., Matthews, A., Frumkin, A., Dayan, U., Halicz, L., Almogi-Labin, A. and Schilman, B.,: Paleoclimate and location of the border between Mediterranean climate region and the Saharo–Arabian Desert as revealed by speleothems from the northern Negev Desert, Israel. E.P.S.L. 249, 384-399, 2006.

Wang, Y.J., Cheng, H., Edwards, R.L., An, Z.S., Wu, J.Y., Shen, C.C., Dorale, J.A.,: A high-resolution absolute dated late Pleistocene monsoon record from Hulu Cave, China. Science 294, 2345-2348, 2001.

Wang, X., Auler, A.S., Edwards, R.L., Cheng, H., Cristall, P. S., Smart, P.L., Richards, D.A. and Shen, C.-C.,: Wet periods in northeastern Brazil over the past 210 kyr linked to distant climate anomalies. Nature 432, 740-743, 2004.

Waugh, D.W., Primeau, F., DeVries, T., Holzer, M.,: Recent changes in the ventilation of the southern oceans Science 339, 568-570, 2013.

Welker, J. M.: Isotopic ($d^{18}O$) characteristics of weekly precipitation collected across the USA: an initial analysis with application to water source studies, Hydrological Processes, 14, 1449-1464, 2000.

Williams, M., Nitschke, N., and Chor, C.: Complex geomorphic response to late Pleistocene climatic changes in the arid Flinders Ranges of South Australia, Geomorphologie, 2006. 249-258, 2006.

Williams, M., Cook, E., van der Kaars, S., Barrows, T.T., Shulmeister, J., Kershaw, P.,: Glacial and deglacial climatic patterns in Australia and surrounding regions from 35 000 to 10 000 years ago reconstructed from terrestrial and near-shore proxy data. Quaternary Science Reviews 28, 2398-2419, 2009.

Wyrwoll, K.-H., Dong, B., and Valdes, P.: On the position of southern hemisphere westerlies at the Last Glacial Maximum: an outline of AGCM simulation results and evaluation of their implications, Quaternary Science Reviews, 19, 881-898, 2000.

Clim. Past Discuss., doi:10.5194/cp-2016-135, 2016
Manuscript under review for journal Clim. Past
Published: 21 December 2016

Climate of the Past
Discussions
Open Access

Table 1: U and Th isotope data and age determinations (in depth order) for stalagmites MC-S1 and MC-S2, Mairs Cave, Flinders Ranges, South Australia. Square brackets indicate activity ratios. MCS2-UM10 was omitted from the age-depth model as it is out of stratigraphic order.

Sample ID (lab no.)[(a)]	*Depth (mm)[(b)]*	*U (ng g^{-1})*	*[^{230}Th/^{232}Th]*	*[^{230}Th/^{238}U][(c)]*	*[^{234}U/^{238}U]*	*Uncorr. age (ka)*	*Corr. age (ka)[(d)]*	*Corr. initial [^{234}U/^{238}U]*
MCS1-UM7(A01962)*	1.0[1.0]	121	1986	0.3766(16)	2.8639(47)	15.15(0.07)	**15.15(0.07)**	2.9453(47)
MCS1-UM8(A01963)*	2.9[1.6]	133	907	0.3826(10)	2.8358(52)	15.57(0.05)	**15.56(0.05)**	2.9182(53)
MCS1-UM3(A01573)*	7.5[0.4]	115	1189	0.3666(13)	2.6761(55)	15.83(0.07)	**15.82(0.07)**	2.7526(56)
MCS1-UM4(A01574)*	32.7[0.4]	115	1271	0.3360(15)	2.3991(48)	16.22(0.08)	**16.22(0.09)**	2.4646(49)
MCS1-UM5(A01575)*	77.6[0.8]	140	2175	0.3295(14)	2.2842(41)	16.75(0.08)	**16.75(0.08)**	2.3463(42)
MCS1-UM6(A01576)*	104.5[1.0]	117	1366	0.3512(15)	2.3819(49)	17.14(0.09)	**17.13(0.09)**	2.4503(51)
MCS2-UM1(A02109)*	2.1[1.5]	74	189	0.2455(26)	1.7728(37)	16.08(0.19)	**16.04(0.19)**	1.8086(38)
MCS2-UM11(D120907-256)	7.8[1.5]	95	43	0.2554(18)	1.6656(48)	17.96(0.15)	**17.73(0.18)**	1.6997(50)
MCS2-UM07(B04007)	8.5[1.0]		15	0.2629(52)	1.6708(66)	18.46(0.40)	**17.82(0.51)**	1.7054(70)
MCS2-UM08(B03992)	11.0[1.7]		54	0.2536(57)	1.6385(94)	18.14(0.45)	**17.97(0.47)**	1.6717(97)
MCS2-UM4(A02778)*	18.9[1.5]	172	793	0.2601(16)	1.6157(28)	18.93(0.13)	**18.92(0.13)**	1.6495(29)
MCS2-UM10(B03993)	21.3[0.8]		58	0.2586(48)	1.6502(100)	18.381(0.39)	**18.22(0.40)**	1.6845(105)
MCS2-UM12(D120907-260)	22.5[1.0]	81	111	0.2707(22)	1.6748(57)	19.00(0.18)	**18.91(0.19)**	1.7118(59)
MCS2-UM05(B03826)	39.5[2.0]	225	636	0.2812(18)	1.6162(34)	20.60(0.15)	**20.58(0.15)**	1.6530(35)
MCS2-UM2(A02110)*	44.3[1.5]	151	27	0.2959(16)	1.6604(30)	21.13(0.13)	**20.72(0.25)**	1.7002(31)
MCS2-UM13(D120907-271)	64.5[1.5]	206	46	0.2987(16)	1.5746(46)	22.65(0.15)	**22.39(0.20)**	1.6121(48)
MCS2-UM06(B03829)	76.4[1.3]	332	10	0.3177(21)	1.5688(33)	24.34(0.19)	**23.02(0.68)**	1.6070(36)
MCS2-UM14(D120907-312)	77.5[1.0]	230	19	0.3098(18)	1.5633(44)	23.77(0.17)	**23.12(0.37)**	1.6013(46)
MCS2-UM15(D120907-404)	94.8[1.5]	273	22	0.3128(16)	1.5203(43)	24.79(0.16)	**24.22(0.33)**	1.5571(45)

(a) Asterisked samples appear in Cohen et al. (2011). Prefix for lab analysis number is "UM".
(b) Median depth from top. Square brackets indicate thickness of calcite wafer.
(c) Figures in brackets are 2-σ uncertainties of the least significant digits.
(d) Age correction is based on $[^{230}Th/^{232}Th]_{initial} = 0.58\pm0.29$; and decay constants given in Cheng et al., 2013.

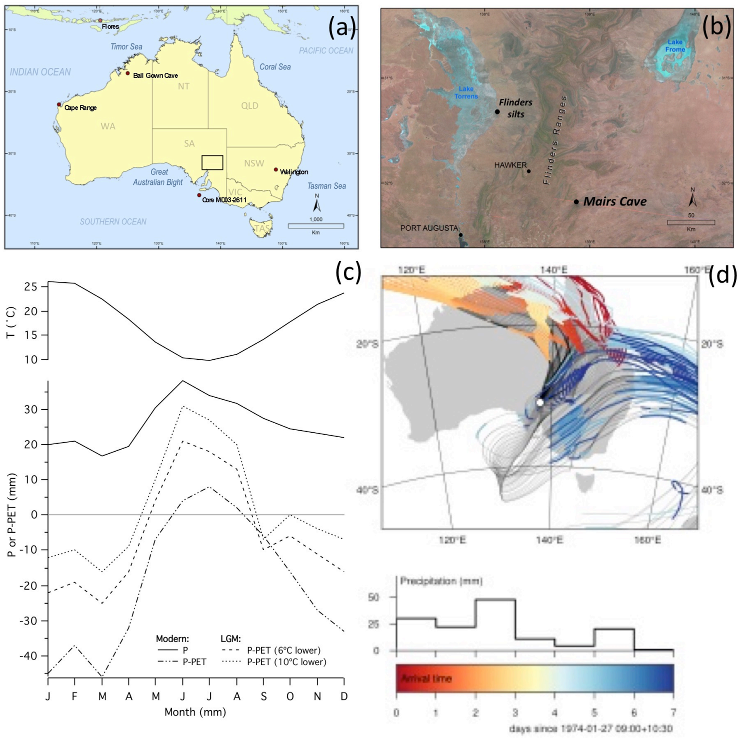

Figure 1a-c: Location of the Flinders Ranges and other sites described in the text (a); location of Mairs Cave, Flinders Silts and Lake Frome (b); monthly climate statistics for Hawker (approximately 60 km from Mairs Cave) and hydrologically effective precipitation or P-PET calculated using the Thornthwaite method for modern day and LGM scenarios of 6 or 10°C temperature cooling (c); and air mass back trajectories for 27/01/1974 to 3/2/1974 (upper panel) and daily precipitation (lower panel) (d). Back trajectories are 10 days long, ending at Mairs Cave and 1500 m AGL. Meteorological forcing is derived from the 2.5° NCEP/NCAR Reanalysis (Kalnay et al., 1996). Trajectories are colour-coded according to arrival time but only during intervals when the airmass is beneath the surface boundary layer to indicate potential moisture sources i.e. we interpret the source of moisture for airmasses arriving between days 4 and 7 to be the Pacific (below boundary layer) rather than the Southern Ocean (above boundary layer). Precipitation is the average of 13 stations within 50 km of Hawker.

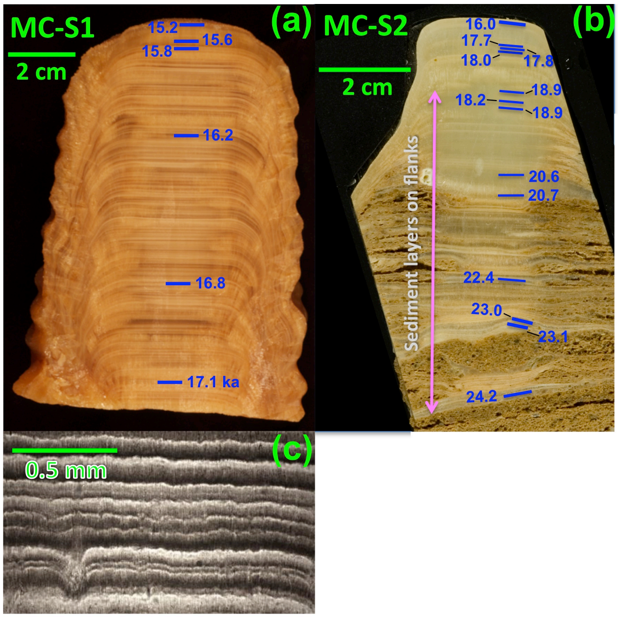

Figure 2a-c: Mairs Cave stalagmites MC-S1 (a) and MC-S2 (b) with age measurements (ka) indicated. Photograph of thin section from MC-S1 at 6 mm below top showing parallel laminae (c). MC-S2 contains layers of sediment interbedded with calcite lenses in its lower half. Sediment continues to be visible on the side flanks until 25 mm below the top coinciding with the age measurement of 18.9 ka. White annulus in layer over 20.6 ka age measurement is a sectioned bone.

Clim. Past Discuss., doi:10.5194/cp-2016-135, 2016
Manuscript under review for journal Clim. Past
Published: 21 December 2016

Climate of the Past Discussions
Open Access

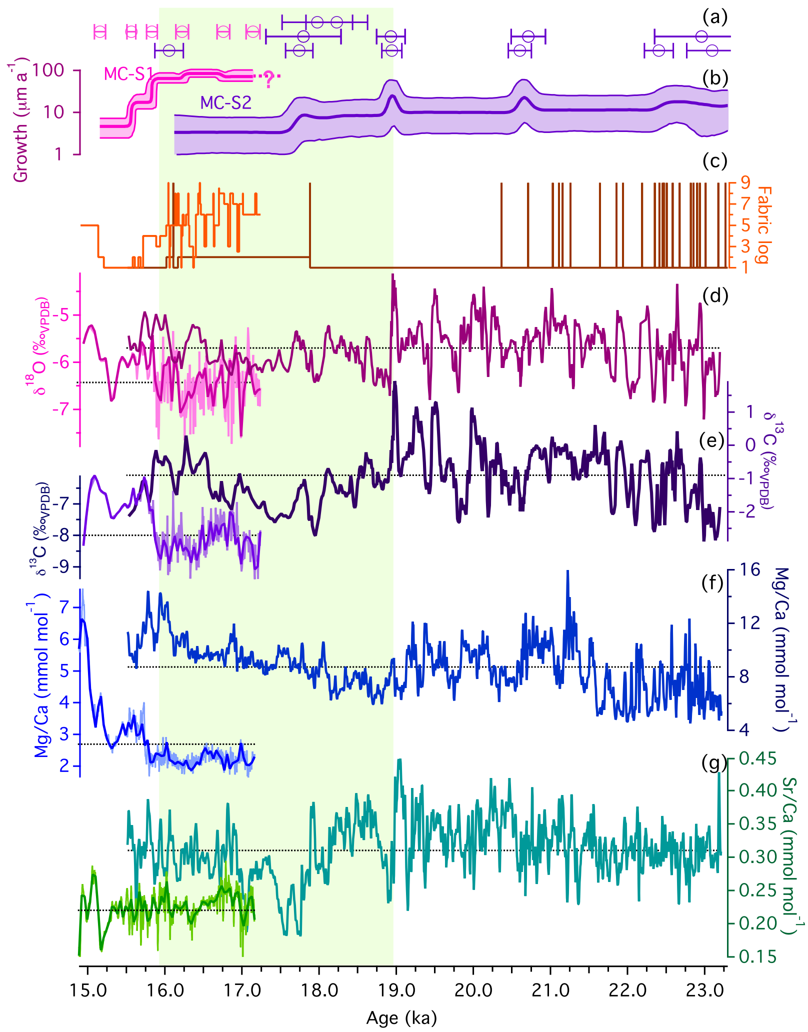

Figure 3: Fig 3a-g: Mairs Cave stalagmites MC-S1 and MC-S2: age measurements (a); growth rate (b); fabric log (c); δ18O (d); δ13C (e); Mg/Ca (f) and Sr/Ca (g). Note different offset scales on left and right-hand axes for panels e to g. Short-lived peaks in growth rate at 19 and 20.6 ka are artifacts of closely-spaced age measurements. Fabric log indicates calcite fabric classification where values 1 to 8 indicate a scale ranging from closed columnar without laminations (=1), to columnar with faint laminations, parallel laminations and rhombohedral tips (=2 to 4), to open columnar calcite (=5), to open columnar with faint laminations, parallel laminations and rhombohedral tips (=6 to 8); 9 marks re-nucleation episodes with geometric selection and possible dissolution. The hierarchy scale suggests increasing discharge and impurities content. Fine dotted line in panels d to g are mean values for each stalagmite. Pale green shading indicates an inferred relatively wetter phase.

Clim. Past Discuss., doi:10.5194/cp-2016-135, 2016
Manuscript under review for journal Clim. Past
Published: 21 December 2016

Climate of the Past Discussions
Open Access
EGU

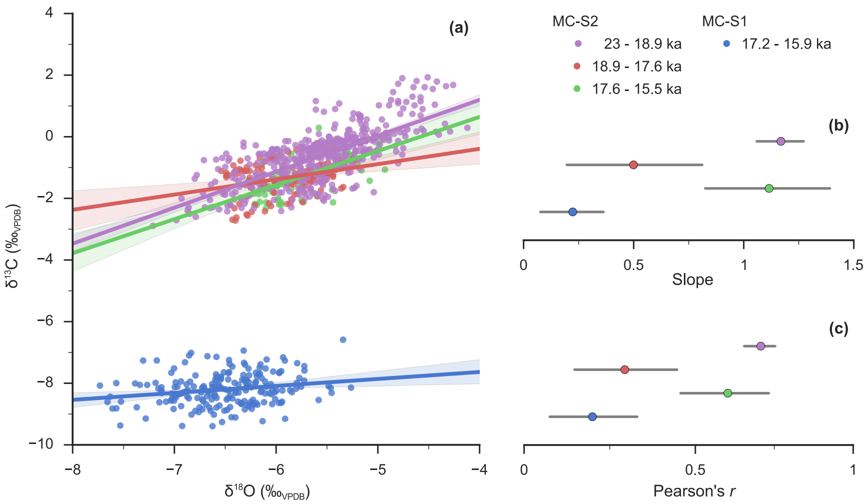

Figure 4a-c: Scatter plot of MC-S1 and MC-S2 $\delta^{18}O$ and $\delta^{13}C$ data for key intervals in the record (a), slopes (b) and r-values (c) for these same intervals. Higher slope and r-values indicate relatively higher isotopic disequilibrium.

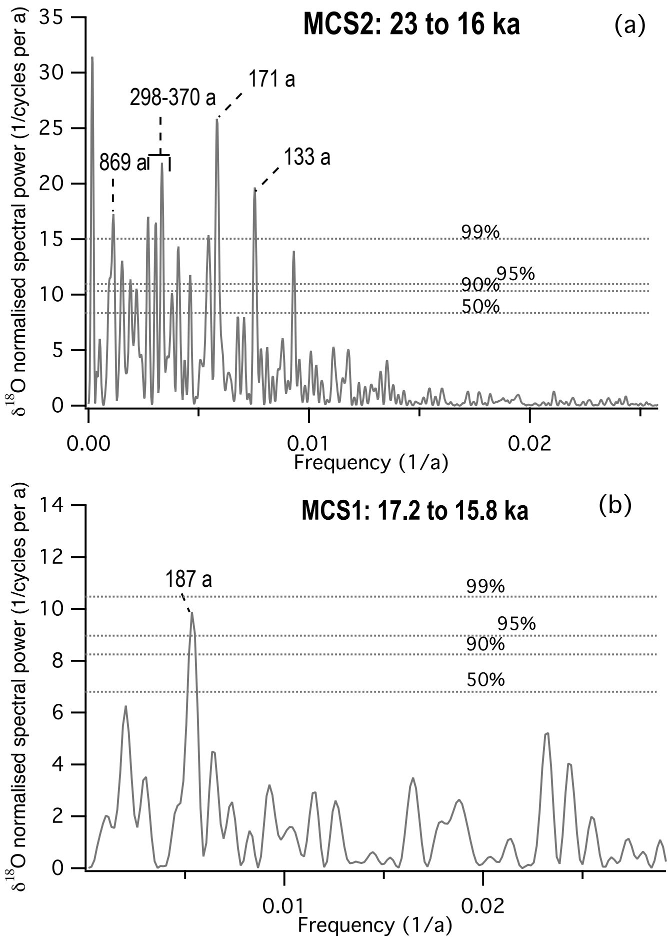

1470
1471 Figure 5a-b: Spectral analysis of MC-S1 and MC-S2 $\delta^{18}O$ between 23.0-15.8 ka
1472 using the Lomb-Scargle method (Press and Rybicki, 1989). Horizontal dotted
1473 lines indicate confidence intervals.
1474

Clim. Past Discuss., doi:10.5194/cp-2016-135, 2016
Manuscript under review for journal Clim. Past
Published: 21 December 2016

Climate of the Past Discussions

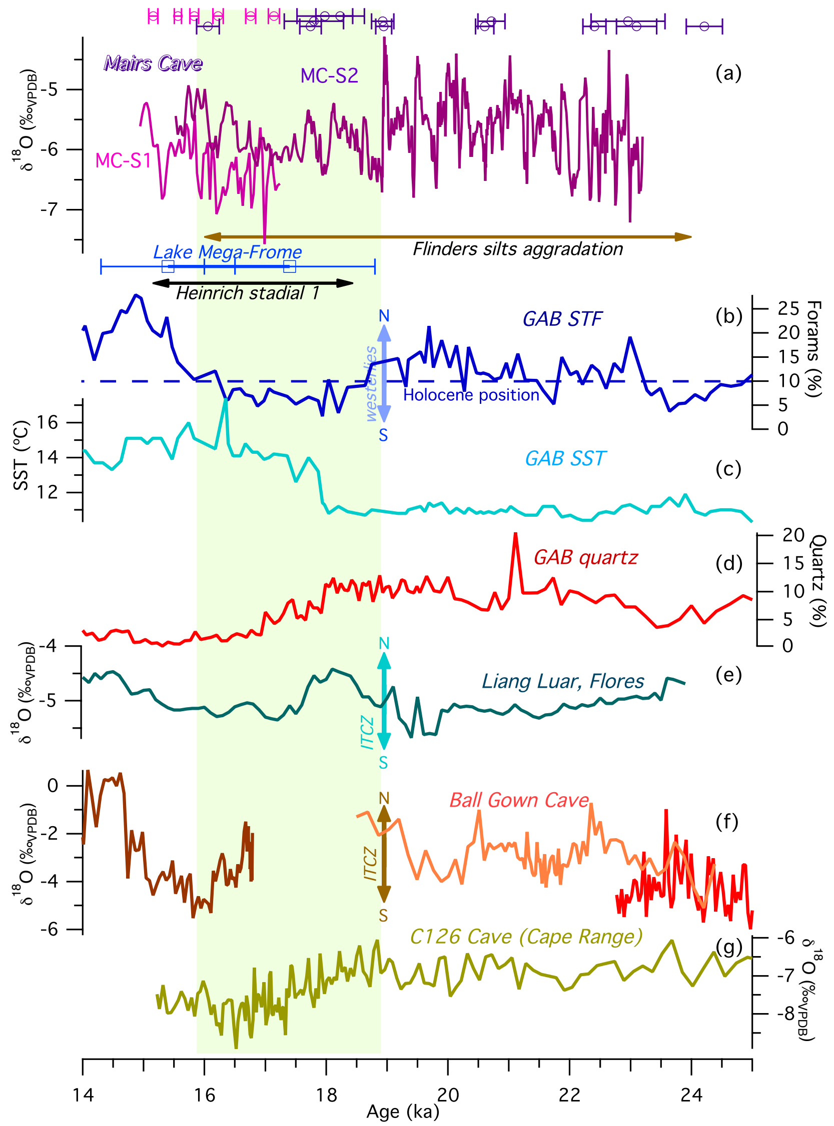

Figure 6: The Mairs cave δ¹⁸O record (a) compared with the foraminifera record (b,c) and the quartz record (d) in marine core MD03-2611 from the Great Australian Bight (DeDeckker et al., 2012); and speleothem records from Liang Luar, Flores (Ayliffe et al., 2013) (e); C126 Cave in Cape Range, Western Australia (Denniston et al., 2013b) (f); and Ball Gown Cave also in Western Australia (Denniston et al., 2013a) (g). The position of the Southern Ocean Subtropical Front and SST are reconstructed from the foraminifera record (DeDeckker et al., 2012).